Forest Ecology and Management 550 (2023) 121478

Contents lists available at ScienceDirect

Forest Ecology and Management

journal homepage: www.elsevier.com/locate/foreco

Consistently heterogeneous structures observed at multiple spatial scales across fire-intact reference sites

Caden P. Chamberlain [a,*], Gina R. Cova [a], C. Alina Cansler [b], Malcolm P. North [c], Marc D. Meyer [d], Sean M.A. Jeronimo [a,e], Van R. Kane [a]

[a] School of Environmental and Forest Sciences, University of Washington, Seattle, WA 98195, USA
[b] W.A. Franke College of Forestry & Conservation, University of Montana, Missoula, MT 59812, USA
[c] USDA Forest Service, Pacific Southwest Research Station, Davis, CA 93546, USA
[d] USDA Forest Service, Region 5 Ecology Program, Southern Sierra Province, Bishop, CA 93514, USA
[e] Resilient Forestry, Seattle, WA 98136, USA

ARTICLE INFO

Keywords:
Reference conditions
Forest structure
Heterogeneity
Lidar
Resilience
Sierra Nevada

ABSTRACT

Yellow pine and mixed-conifer (YPMC) forests of California's Sierra Nevada have experienced widespread fire suppression for over a century, resulting in ingrowth and densification of trees, heavy fuel accumulation, and shifts in species composition. Under warmer and drier climates, these forests are primed for stand-replacing fires and severe drought mortality, requiring management interventions to improve their resilience and mitigate future impacts. Observations from functioning frequent-fire systems (e.g., contemporary reference sites) can provide key insights about pattern-process relationships in fire-intact systems, which can be used to inform regional management efforts. In this study, we used airborne lidar data to quantify and compare forest structure at multiple spatial scales between contemporary reference sites (i.e., forests with a restored frequent, low-intensity fire regime) and control sites (i.e., typical fire-suppressed forests). We evaluated structures at the neighborhood- (~1 ha), site- (~100–1,000 ha), and among-site- (~10,000–100,000 ha) levels. In reference sites, high proportions of individual trees, small clumps of 2–4 trees, and open space formed mostly open canopy structures at the neighborhood-level, and patches of these neighborhood-level structures were arranged in heterogeneous spatial patterns within sites. We observed low variability in site-level structures *among* reference sites, indicating a stabilizing effect of frequent, low-intensity fire across broad, ecosystem scales. In fire-suppressed control sites, edaphic factors and other non-fire disturbances occasionally produced heterogeneity at the neighborhood- and site-level, but the degree of heterogeneity was not consistent across sites. Structural patterns in contemporary reference sites suggest improved resilience to future disturbances and climate change, and increased provisioning of ecosystem services relative to control sites. We suggest applying these metrics to help inform multi-scale and multi-resource management in Sierra Nevada forests.

1. Introduction

For centuries, fire has played a key role in shaping the structure and composition of the yellow pine and mixed-conifer (YPMC) forests of California's Sierra Nevada (North et al., 2016; Safford and Stevens 2017). Prior to Euro-American colonization, lightning ignitions and Indigenous burning practices maintained a frequent (<20-year fire return interval), low-intensity fire regime, supporting mostly low-density forest structures and dominance of large fire-tolerant trees (Stephens et al., 2015; Taylor et al., 2016; Safford and Stevens 2017; North et al., 2022). Historical YPMC forests represented an archetypical example of ecosystem resilience by maintaining a stable range of structure and composition through centuries of repeat fires, climatic variability, and other disturbances (Walker et al., 2004; Hessburg et al., 2019; Ziegler et al., 2021).

Beginning in the late 1700s, Euro-American colonization led to disruption of Indigenous burning, extensive logging and livestock grazing, and widespread fire suppression, over time resulting in increasingly dense and fuel-loaded forests (Knapp et al., 2013; Taylor et al., 2016; Safford and Stevens 2017; Hagmann et al., 2021). With

* Corresponding author at: Anderson Hall, 3715 W Stevens Way NE, Seattle, WA 98195, USA.
E-mail address: cc274@uw.edu (C.P. Chamberlain).

https://doi.org/10.1016/j.foreco.2023.121478
Received 5 May 2023; Received in revised form 2 October 2023; Accepted 3 October 2023

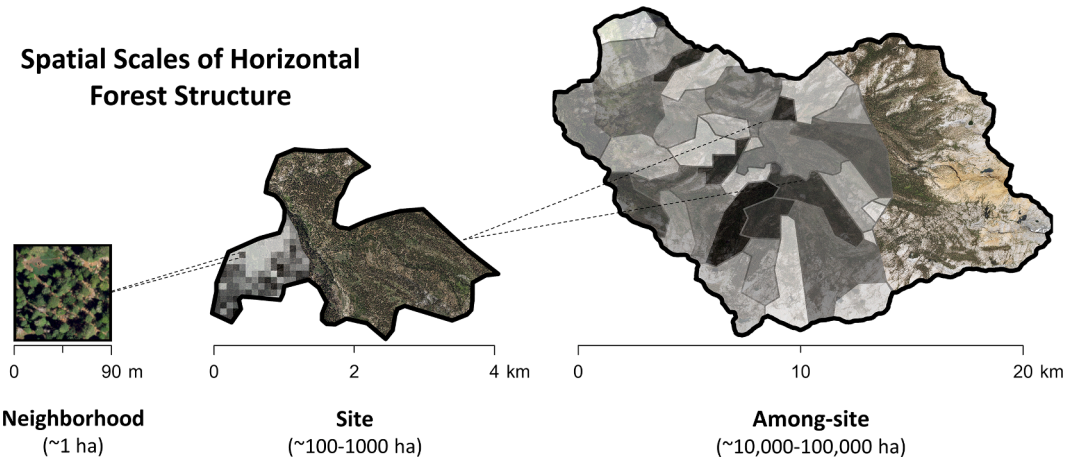

Fig. 1. Conceptual diagram showing the three nested spatial scales explored in this study including neighborhood-level (~1 ha pixel), site-level (~100–1,000 ha), and among-site-level (~10,000-100,000 ha). True color National Agriculture Imagery Program (NAIP) imagery shown in background for each spatial scale.

warmer and drier climatic conditions in the 21st century, these contemporary forests are susceptible to uncharacteristically severe wildfires and droughts (Steel et al., 2015; Restaino et al., 2019; Williams et al., 2019), often with enormous environmental and social consequences (Coop et al., 2020; Safford et al., 2020; Schulze et al., 2020; Meigs et al., 2023).

Management efforts across much of the Sierra Nevada are focused on improving resilience to fire, drought, and climate change, while also protecting or enhancing key ecosystem services like wildlife habitat and biodiversity (North et al., 2009, Stephens et al., 2016a; Safford and Stevens 2017; Stephens et al., 2021; Forest Management Task Force, 2021). Observations of structural patterns from functioning frequent-fire forests are critical to informing management efforts in pursuit of these broad objectives (Keane et al., 2009; Hessburg et al., 2015; Collins et al., 2016; Jeronimo et al., 2019; Wiggins et al., 2019). Such observations offer important insights about pattern-process relationships in fire-intact ecosystems which are essential to the successful design and implementation of resilience-focused and multi-resource management (North et al., 2009; Larson and Churchill 2012; Churchill et al., 2013; Hessburg et al., 2015; Jeronimo et al., 2019).

Historical datasets and reconstruction studies have provided many detailed descriptions of structural conditions in frequent-fire forests prior to Euro-American colonization (e.g., Collins et al., 2011; Larson and Churchill 2012; Lydersen et al., 2013; Safford and Stevens 2017). While these datasets offer extensive information about finer-scale structures (i.e., neighborhood- to stand-level) they typically lack thorough and quantitative descriptions about coarser-scale structures and spatial patterns (i.e., site- to watershed-level) (Fig. 1). However, characterizing structural patterns at these coarser-scales is essential, since pattern-process relationships often unfold across multiple, interacting scales and because multi-resource management (i.e., fire resistance at the tree-scale and wildlife habitat across landscapes) is inherently multi-scaled (Stephens et al., 2016b; Falk et al., 2019; Koontz et al., 2020; Falk et al., 2022; Loudermilk et al., 2022).

In recent decades, several sites across the Sierra Nevada have experienced multiple overlapping fires with low- to moderate-severity effects (<75 % tree mortality). These sites – often termed contemporary reference sites – represent forests where a frequent, low-intensity fire regime has begun to reestablish after decades of fire suppression (Collins et al., 2009; Collins et al., 2016; Jeronimo et al., 2019; Pawlikowski et al., 2019; Wiggins et al., 2019; Ng et al., 2020). Contemporary reference sites provide important opportunities to measure and analyze multi-scale structural patterns in 21st century fire-intact systems. These characterizations are especially enhanced where high-fidelity and spatially extensive remote sensing datasets, like airborne lidar, are available (Jeronimo et al., 2019; Wiggins et al., 2019). Contemporary reference sites also have the advantage of representing forests that have developed, at least partially, under modern climate conditions; thus, structural observations from these sites can be used to inform forward-looking, climate-smart management strategies (Lydersen and North 2012; Churchill et al., 2013; Collins et al., 2016; Jeronimo et al., 2019; Wiggins et al., 2019).

Ecological resilience can be defined as the capacity of ecosystems to withstand or recover from common disturbances and climatic variability while maintaining a relatively stable range of structure and composition across relevant time scales (Walker et al., 2004). Some researchers (Westman 1978; Carpenter et al., 2001; DeRose and Long 2014) have suggested that definitions of resilience must specify resilience of what and to what, at appropriate spatial and temporal scales. Therefore, in this study, we define resilience as the ability of YPMC forests to retain their structure, composition, and functional integrity in response to stresses common to this forest type (e.g., fire, drought, and insects) at the ecosystem scale and over the age span of the dominant trees (i.e., 300–400 years).

Indicators of resilience describe the mechanisms that enable forests to either withstand or recover from disturbances (Falk et al., 2022). At the neighborhood-level (Fig. 1), arrangements of individual trees, small clumps of trees, and open space (an ICO pattern) can indicate increased resilience in YPMC forests, as these patterns can mitigate fire-induced mortality of dominant trees while also reducing competition and increasing drought tolerance (Larson and Churchill 2012; Ziegler et al., 2017; Ritter et al., 2020; Ziegler et al., 2021; Atchley et al., 2021). At the within-site-level (Fig. 1), heterogeneity in forest patch densities may also indicate improved resilience, as variability in forest densities can reduce the likelihood of large high severity burned areas which can inhibit post-fire seed dispersal and recovery (Hessburg et al., 2019; Coop et al., 2020; Francis et al., 2023). Researchers have also theorized that low-intensity and frequent fire regimes historically represented a strong top-down control on forest structure across broad spatial scales (e.g., Larson and Churchill 2012; Knapp et al., 2017). Thus, resilience among-sites (Fig. 1) may best be characterized as a *consistency* in finer-scale heterogeneity, due to the pervasive top-down influence of low-intensity and frequent fire regimes.

We currently lack a comprehensive analysis of structural patterns across multiple, hierarchical scales in contemporary reference sites of the Sierra Nevada. Past studies have proposed a conceptual model of a nested hierarchical structure in frequent-fire forests prior to Euro-American colonization – where neighborhood-level tree clump and opening patterns scaled up to produce heterogeneous patch arrangements within stands and sites, together supporting resilience across

ecosystems (Bonnicksen and Stone, 1980; Larson and Churchill, 2012; Reynolds et al., 2013; Collins et al., 2015; Hessburg et al., 2019). Now, with recent and extensive collections of high-fidelity airborne lidar covering large extents of the Sierra Nevada, including many contemporary reference sites, this hierarchical ecosystem structure can be empirically quantified and analyzed. Such structural characterizations will provide essential diagnostics that can be used when managing for resilience and other ecosystem services across the region (North et al., 2009; Churchill et al., 2013; Hessburg et al., 2015; Greiner et al., 2020).

In this study, we analyzed forest structural patterns across contemporary reference sites (hereafter, reference sites) at multiple spatial scales in the Sierra Nevada YPMC zone and compared these structures against control sites representing fire-suppressed forests. Our comparisons of structures between fire-intact reference sites and fire-suppressed controls sites allowed us to identify the effects of frequent-fire while controlling for topographic, climatic, and productivity influences. We used airborne lidar data (hereafter 'ALS') to quantify a scalable set of horizontal forest structure metrics at three spatial scales including 1) neighborhood-level tree clump and opening patterns, 2) within-site patch arrangements, and 3) among-site variability (Fig. 1).

We sought to address two primary objectives in our analyses:

1) Identify and classify the diversity of horizontal forest structures across reference and control sites at the neighborhood-level (~1 ha) and aggregate these measures to quantify site-level (~100–1,000 ha) and among-site-level structural patterns (~10,000-100,000 ha).
2) Compare structures between reference and control sites at each spatial scale to discern key structural patterns produced by a contemporary, frequent, and low-intensity fire regime.

2. Methods

2.1. Study area

California's Sierra Nevada is characterized by a Mediterranean climate in which approximately 85% of precipitation falls between November and May and summer months are consistently dry. Interannual fluctuations in climate are largely driven by El Niño-Southern Oscillation (ENSO) patterns causing general shifts from wetter to drier periods every 3–5 years (North et al., 2016). Broad-scale topographic factors result in higher precipitation, cooler temperatures, and more persistent snowpack at higher elevations and latitudes, while fine-scale topography influences variability in plant water availability and solar radiation (North et al., 2016; van Wagtendonk et al., 2018). Soils in the western Sierra Nevada are generally young, acidic, and have relatively deep organic horizons (North et al., 2016; van Wagtendonk et al., 2018).

Yellow pine and mixed-conifer (YPMC) forests cover nearly 3 million ha of the Sierra Nevada ecoregion (EPA Ecoregions, 2023), and represent an area of high ecological, social, and economic importance (Safford and Stevens 2017). Major tree species in the YPMC zone include ponderosa pine (*Pinus ponderosa*), Jeffrey pine (*Pinus jeffreyi*), sugar pine (*Pinus lambertiana*), Douglas-fir (*Pseduotsuga menziesii*), white fir (*Abies concolor*), red fir (*Abies magnifica*), incense cedar (*Calocedrus decurrens*), and black oak (*Quercus kelloggii*). We used the FVEG dataset to define the specific boundaries of the YPMC zone. The FVEG dataset provides 'best available' landcover type maps for California for years approximately 1990–2014 (FVEG, 2015). We focused our analyses on the FVEG Wildlife Habitat Relationship (WHR) classes including Montane Hardwood-Conifer, Ponderosa Pine, Jeffrey Pine, Douglas Fir, and Sierran Mixed Conifer, which generally align with YPMC forest types described in Safford and Stevens (2017).

Prior to Euro-American colonization beginning in the 1700s, YPMC forests were characterized by a frequent, low intensity fire regime driven by natural lightning ignitions and Indigenous burning (Anderson and Moratto, 1996; Safford and Stevens, 2017). The historic mean fire return interval was 11–16 years with most fire resulting in low- and moderate-severity effects and only about 8–15% high-severity effects (Safford and Stevens 2017). Across broad temporal scales (i.e., millennia), droughts historically occurred every 80 to 260 years with most droughts lasting 20 to 100 years (Safford and Stevens 2017). Major droughts led to increased moisture stress on trees which subsequently led to periodic and isolated insect outbreaks and tree mortality (North et al., 2016; Safford and Stevens 2017).

Sierra Nevada forests are managed by a variety of private landowners and local, state, and federal agencies. Most forests fall under the jurisdiction of the United States Forest Service (FS) where, outside of wilderness areas, they are managed for multiple resources including timber, wildlife, water protection, and recreation (North et al., 2009). A considerable proportion of the Sierra Nevada is also managed by the National Park Service (NPS) where management is centered on preservation and recreation (Allen et al., 2019; Wood and Jones 2019). Current NPS and FS wilderness policies, as well as federal fire management policy guidance, permit lightning-ignited fires to be managed for resource objectives as specified in land or resource management plans, yet most ignitions are still typically suppressed (van Wagtendonk 2007; Massip 2020; Young et al., 2020).

2.2. Reference and control sites

Across the Sierra Nevada YPMC zone, we sought to compare forest structural patterns at multiple scales between reference sites (i.e., sites with repeat low/moderate-severity fire effects) and control sites (i.e., fire-suppressed forests with no recent fire activity). We followed an approach initially developed by Jeronimo et al. (2019) to identify a set of reference sites for our study. Here we provide a summary of this approach, with additional detail provided in an associated Data in Brief publication (Chamberlain et al., 2023a, *in review*) and in the metadata for the archived dataset (https://doi.org/10.2737/RDS-2023-0027; Chamberlain et al., 2023b). The general approach for identifying reference and control sites involved 1) scoring rasters across our study area based on the degree to which each 30 m pixel represented either a restored fire regime (for reference sites) or fire-suppressed forests (for control sites), and 2) defining site polygons around clusters of high scoring pixels using the national catchment dataset (NHDPlusV2, 2021) along with fire perimeters, burn severity layers, and ESRI imagery.

2.2.1. Datasets

We used fire history datasets to identify areas with a restored frequent, low-intensity fire regime (reference sites) or areas with no recent fire history (control sites). We used CALFIRE's Fire Resource and Protection Program (FRAP) fire history dataset to map all fires occurring in the YPMC zone from 1957 to 2020 (FRAP Fire Perimeters, 2021; Cova et al., 2023). Records for all fires >4 ha including prescribed burns were included. We used the Parks et al. (2019) Google Earth Engine script to quantify and map predicted Composite Burn Index (CBI) burn severity for all fires intersecting our study area (see detailed methods in Cova et al., 2023). Thresholds recommended by Miller and Thode (2007) were used to classify continuous CBI rasters into categories of unburned-, low-, moderate-, and high-severity. Prior to 1985, Landsat data was not available for modeling burn severity. Thus, for all pre-1985 fires in our dataset that intersected potential reference sites, we visually examined imagery and a lidar-derived canopy height layer (more detail below) for evidence of past stand-replacing fire and excluded all expected high-severity burn areas from our analyses.

We mapped management history to ensure that neither reference nor control sites had been impacted by treatments or harvest in recent decades. We used 1) a dataset developed by Knight et al. (2022) for years 1985–2020 and 2) the Forest Service FACTS database for years prior to 1985 (USDA FACTS, 2021). The Knight et al. (2022) dataset provides a compiled and organized record of treatment history across private, state, and federal lands for years 1985–2020. Tables provided in the Knight et al. (2022) supplemental materials (Tables S4-S8) were used to classify

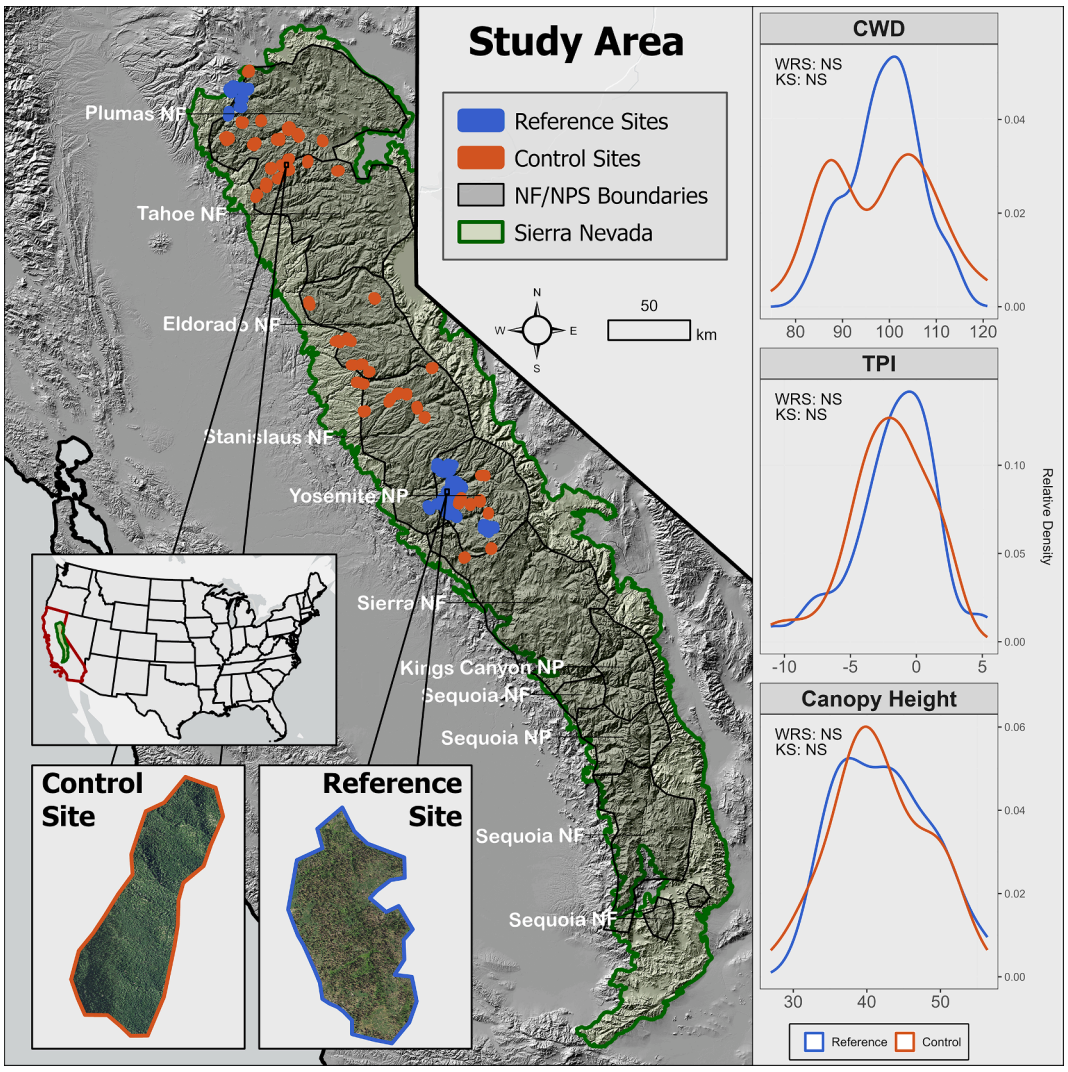

Fig. 2. California's Sierra Nevada ecoregion defined by the Environmental Protection Agency's Level IV Ecoregions dataset (EPA Ecoregions, 2023) with all intersecting National Forest (NF) and National Park Service (NPS) administrative boundaries (smoothed for visualization). Geographic distribution of reference (blue) and control (orange) sites used in analyses with example of each site type (left). Density curves for climatic water deficit (CWD), canopy height, and 2000 m topographic position index (TPI) compared between reference and control sites (right). No significant differences ($\alpha > 0.05$) found in median (Wilcoxon Rank Sum, WRS) or distribution (Kolmogorov-Smirnov, KS) between climate, canopy height, or topographic indices between reference and control sites.

and discard records representing administrative, monitoring, and prescribed burning tasks. For years prior to 1985, we relied solely on the USDA Forest Service FACTS dataset to track treatment history on federal lands and used the same tables from Knight et al. (2022) supplemental materials to classify and discard administrative-, monitoring-, and fire-related treatments.

We used the FVEG forest type dataset to ensure that both reference and control sites represented primarily YPMC forests. The Landscape Change Monitoring (LCMS) dataset was used to identify and exclude areas impacted by non-fire disturbances in our control sites (Housman et al., 2022). Lastly, the national catchment dataset (NHDPlusV2, 2021) and ESRI imagery (ESRI World Imagery, 2021) were used to delineate individual site boundaries (more detail provided below).

2.2.2. *Identifying reference and control sites*

We followed methods initially presented in Jeronimo et al. (2019) to identify reference sites for our analyses. We implemented a raster scoring approach in which each 30-m pixel in a representative raster across our study area was scored based on the degree to which it represented a restored low-intensity, frequent fire regime in the YPMC zone. Specifically, each pixel was given a point for 1) at least 2 fires in the last 60 years, 2) at least one fire in the last 30 years, 3) at least one fire with moderate-severity effects, 4) no high-severity effects, 5) no record of late 20th or early 21st century timber management, and 6) representing one of the desired FVEG YPMC forest types (defined in Section 1.1.). Specific site boundaries were then defined using the national catchment dataset (NHDPlusV2, 2021). We selected all catchments that were dominated by 'score 6′ cells and were >100 ha in size. We then made minor manual adjustments to selected catchment boundaries using fire perimeters, burn severity rasters, and ESRI imagery to ensure that our sites represented primarily forested areas and excluded roads, infrastructure, and major rock outcrops. Detailed methods are provided in an associated Data in Brief manuscript (Chamberlain et al., 2023a, *in review*) and the metadata for the archived dataset (https://doi.org/10.2737/RDS-2023-0027; Chamberlain et al. 2023b). We identified 119 reference sites and described and quantified their characteristics in the aforementioned paper.

For this study, we reduced and focused the reference site datasets to sites where ALS data was collected at least 5 years following the most recent fire (see details on ALS data in Section 2.1.). This selection criterion was applied to improve quantification of *live* forest structure metrics (as recent drought and extensive wildfires have driven

Table 1
Total area, count, and mean, maximum, and minimum size for reference and control sites.

Site Type	Total Area (ha)	# Sites	Mean Size (ha)	Max Size (ha)	Min Size (ha)
Reference	11,850	42	282	841	102
Control	10,031	42	238	692	114

widespread tree mortality across the region (Steel et al., 2022)) and to ensure more reliable comparisons of structural patterns between reference and control sites. Five years was selected based on rates of post-fire mortality identified by van Mantgem et al. (2011) and Jeronimo et al. (2020). We acknowledge that this criterion did not guarantee removal of all snags prior to quantifying forest structure metrics; instead, it minimized the impact of snags while maintaining a large sample of sites upon which we could draw ecological inferences. Nevertheless, we acknowledge that trees that died and/or snags that remained standing >5 years post-fire had some influence on ALS metrics.

To identify a set of control sites representing typical fire-suppressed forests, we applied a raster scoring approach similar to that used to identify reference sites. Specifically, each 30-m pixel across our study area was given a point for each of the following true statements: 1) no fire history, 2) no record of late 20th or early 21st century timber management, and 3) no "Fast Change" detected by the LCMS dataset (Housman et al., 2022). The LCMS criterion was applied to ensure that control sites had not been heavily affected by other sudden non-fire disturbances in recent decades (Housman et al., 2022). Then, using the same method for defining reference sites, we selected all catchment polygons (NHDPlusV2, 2021) with majority 'score 3' pixels that were >100 ha, then used fire perimeters, burn severity layers, and ESRI imagery to make minor adjustments to polygons to ensure control sites represented forested areas and excluded roads, infrastructure, and major rock outcrops.

The reference and control site datasets were further filtered to ensure that observed differences in forest structure between the site types were indeed the result of fire and fire-suppression, respectively, rather than differences in climate, topography, or forest age. Specifically, we compared distributions of climatic water deficit (CWD) (Flint et al., 2021), topographic position index (TPI), and ALS-derived canopy height (a proxy for stand age, more detail provided below) between the site types. We first observed the distributions of CWD, TPI, and canopy height between the reference and control sites and removed sites from our analyses that clearly represented outlier climate, topographic, or stand age conditions (e.g., mean canopy height <20 m). Then, we used Wilcoxon Rank Sum (WRS) and Kolmogorov-Smirnov (KS) tests to confirm no significant differences ($\alpha > 0.05$) in the median or distribution, respectively, of mean site-level CWD, TPI, or canopy height between the reference and control sites (Fig. 2) (Gotelli and Ellison 2018). Scatter plots showing the distributions of reference and control sites across CWD, TPI, and canopy height are also provided in Appendix Fig. A1. After applying these filters, we had a final set of 42 reference sites and 42 control sites. Final reference and control site metrics are provided in Table 1. The lack of reference and control sites in the southern Sierra is primarily due to the lack of ALS datasets that met the 5-year post-fire criterion. Reference sites are publicly available on the Forest Service Research Data Archive (https://doi.org/10.2737/RDS-2023-0027; Chamberlain et al., 2023b), and control site boundaries are available on the Zenodo Digital Repository (https://doi.org/10.5281/zenodo.8401035).

2.3. Tree clump and opening metrics with ALS

We used high fidelity airborne laser scanning (ALS) data to quantify and compare a multi-scale set of forest structure metrics between reference and control sites. ALS data is currently available for large portions of the Sierra Nevada YPMC forests. For this study, we used six primary acquisitions that were collected between 2018 and 2020 including North and South Plumas National Forest, Eldorado National Forest, Tuolumne County, Yosemite National Park, and the Southern Sierra All Resource Restoration (SSARR) project area. These ALS acquisitions were each collected via aircraft during leaf-on months and provide high fidelity, georeferenced point cloud and ground model datasets. The ALS data met minimum pulse density and flight line overlap standards recommended for performing forest structure-based analyses (Gatziolis and Andersen 2008). Details for each acquisition are provided in Table 2.

Table 2
Information for six airborne lidar (ALS) acquisitions including acquisition name, year(s) flown, total area, mean pulse density/m^2, and average flight line overlap. SSARR refers to Southern Sierra All Resource Restoration project area.

Acquisition Name	Years Flown	Total Area (ha)	Mean Pulse Density (pulse/m^2)	Average Flight Line Overlap
North Plumas NF	2018	466,774	13.3	>50 %
South Plumas NF	2018	560,370	12.6	>50 %
Eldorado NF	2019	577,109	28.0	>50 %
Tuolumne County	2018/2019	694,330	15.3	>50 %
Yosemite NP	2019	369,824	23.5	>50 %
SSARR	2020	569,810	22.0	>50 %

We used the USDA Forest Service's FUSION software to process all six ALS acquisitions. Primary steps included 1) normalizing return heights, 2) producing canopy height models, 3) segmenting trees, and 4) deriving structure metrics from segmented trees (McGaughey, 2020). Using FUSION's Lidar Toolkit, we first used vendor-provided ground models to normalize each ALS acquisition so that Z coordinates represented vegetation height above ground. The resultant normalized point clouds were then used to produce 0.75-m resolution canopy height models (CHMs). CHMs were smoothed using a 3×3-cell mean filter to reduce the effects of noise on the tree segmentation algorithm (Jeronimo et al., 2018). CHMs were further filtered to remove all cells <2 m so that derived structure metrics were representative of overstory tree structures rather than shrubs or other understory vegetation.

Individual trees were segmented in FUSION using the watershed algorithm (Vincent and Soille 1991), a computationally efficient algorithm that is widely used in other ALS-based forest structure research (Jeronimo et al., 2018). After applying the algorithm, FUSION produced an X and Y coordinate for each tree, a maximum tree height value, and a polygon representing the approximate crown dimensions of each tree. Past work has demonstrated that ALS-segmented trees are not fully representative of on-the-ground trees since many of the subcanopy trees are not identified in the segmentation process (Richardson and Moskal 2011; Jeronimo et al., 2018; Wiggins et al., 2019). Thus, we hereafter refer to all ALS-segmented trees as Tree Approximate Objects (TAOs) to explicitly recognize the limitations of segmentation algorithms while facilitating the production of ecologically meaningful metrics (Jeronimo et al., 2018, 2019).

We produced a set of ICO (individual tree, clump, and opening) and canopy height metrics from the ALS-derived TAOs that are known to be important metrics related to resilience in historically frequent-fire forests (Larson and Churchill 2012; Churchill et al., 2013; Lydersen et al., 2013). We followed methods from past work to produce ALS-derived ICO metrics (Jeronimo et al., 2019; Kane et al., 2019; Wiggins et al., 2019). All metrics were computed at 90-m resolution (~1-ha) as this is the approximate scale at which fine-scale tree spatial patterns are known to emerge in frequent-fire forests (Larson and Churchill 2012). TAOs were considered part of the same clump if their estimated crown polygons overlapped. Within each 90-m pixel, we computed the percent total canopy area occupied by individual TAOs and clumps of 2–4, 5–9, and

Table 3
Name, abbreviation, description, interpretation, and range for four heterogeneity indices including aggregation index, interspersion-juxtaposition index, area-weighted mean patch size, and Shannon's evenness index. Table adapted from Cova et al. (2023) and Singleton et al. (2019).

Metric	Abbreviation	Description	Interpretation of Low Values	Interpretation of High Values	Range (units)
Aggregation Index	AI	Likelihood that pixels from one class are adjacent to pixels of the same class	Low clumping of pixels of the same class	High clumping of pixels of the same class	0–100 (unitless index)
Interspersion-juxtaposition Index	IJI	Describes the degree to which the edge of patches are likely to be adjacent to all other patch types (high value) or only one other patch type (low value)	Low intermixing of patch types	High intermixing of patch types	0–100 (unitless index)
Area-weighted mean patch size	AWMPS	Mean area of patches weighted by relative patch size within each site	Pixel chosen at random will belong to small patch	Pixel chosen at random will belong to large patch	0.81–427 (ha)
Shannon's Evenness Index	SHEI	Degree of similarity in proportions of classes	Distributions are not even, and a few classes dominate	Distributions are even, and no single class dominates	0–1 (unitless index)

10 + TAOs. We also computed a percent area gap metric as the percentage of area within the pixel not occupied by TAO crowns. Lastly, we computed the 95th percentile of TAO heights (i.e., 'canopy height') within each pixel.

We applied the above workflow to each of the six ALS acquisitions to derive a final set of 90-m resolution ICO and height metrics spanning the reference and control sites. Lastly, we mosaicked rasters across acquisitions into a final set of rasters with uniform spatial resolutions (90-m) and projections (EPSG: 3310) to enable cross-acquisition comparisons of structure.

2.4. Neighborhood-level structure

Analysis of individual ICO metrics can be challenging to interpret and difficult to translate into straightforward, operational management objectives and evaluation metrics (North et al., 2022). Thus, we used hierarchical clustering to produce a set of horizontal structure classes from the ICO structure metrics to 1) produce outputs that could be more easily interpreted for management applications and 2) could be aggregated to characterize broader site-level structures. We defined a set of structure classes for all pixels intersecting the reference and control sites described above (Section 1.2.). Hierarchical clustering algorithms can quickly overwhelm computer memory when building distance matrices, so we first performed clustering on a random stratified sample of 27,000 pixels, then produced a Random Forest model to predict the resultant structure classes for all pixels across the reference and control sites.

We stratified pixels using the percent area gap and the 95th percentile of TAO height metrics (described above) to ensure that our sample captured a range of forest conditions. We then applied an unsupervised agglomerative hierarchical clustering algorithm using a Euclidean distance measure on all ICO metrics (i.e., % area gap, % single TAOs, and % 2–4, 5–9, and 10 + TAO clumps) to define a set of horizontal structure classes (Gotelli and Ellison 2018). To determine the most ecologically meaningful and statistically distinct number of structure classes (i.e., where to "prune" the resultant dendrogram), we evaluated a dendrogram (Fig. 1) and scree plot (Appendix Fig. A2) from the hierarchical clustering analysis and analyzed the distribution of input metrics in different class combinations. After deciding on the number of structure classes, we produced a Random Forest classification model using the ICO metrics as explanatory variables and the structure classes as a response and applied this model to predict the structure class of all pixels across the reference and control sites (Cutler et al., 2007). All analyses were performed in R (R Core Team, 2023) using the *terra* (Hijmans et al., 2023) and *randomForest* (Liaw and Wiener, 2002) packages and other base R functions. We used default parameters for the Random Forest model.

2.5. Within- and among-site-level structure

Fine-scale forest structure patterns (i.e., neighborhood-level structure classes) describe a key spatial scale of forest structures in frequent-fire forests (Larson and Churchill 2012); however, it is also useful to quantify and analyze coarser scale structural patterns (i.e., within- and among-sites) to better inform management and understand repeat fire effects at these broader spatial scales (Turner and Romme 1994; Larson and Churchill 2012; Hessburg et al., 2019; Francis et al., 2023). For example, site-level heterogeneity indices including patch size or spatial aggregation metrics can provide key information about the proportions and spatial configurations of finer-scale structures across a site (McGarigal and Marks 1995; He et al., 2000; Hessburg et al., 2000). Furthermore, measuring among-site variability in heterogeneity metrics can provide information about the consistency of patterns across broader spatial scales (i.e., multiple sites). Thus, to analyze these coarser spatial scales, we quantified and compared 1) within-site heterogeneity indices of the finer-scale structure classes (described in section 1.4.) and 2) among-site variability of these site-level indices.

We first derived the proportions of each structure class by site type (reference vs. control) and compared these distributions to identify dominant patterns of fine-scale structures. Next, we characterized site-level heterogeneity and spatial configurations of forest structure using a parsimonious set of heterogeneity indices (Cushman et al., 2008) including aggregation index (AI), interspersion-juxtaposition index (IJI), area-weighted mean patch size (AWMPS), and Shannon's evenness index (SHEI) (McGarigal and Marks 1995; He et al., 2000). Aggregation index describes the likelihood that pixels are adjacent to pixels of the same class and provides a measure of "clumpiness" across a site (He et al., 2000). Interspersion-juxtaposition index is referred to as the "salt and pepper" index and ranges from 0 to 100. A value of 0 suggests that classes, on average, are only adjacent to patches of a single other class type, while a value of 100 suggests that classes, on average, are equally adjacent to patches of all other class types. Area-weighted mean patch size describes the average patch size that a randomly selected pixel belongs to, and thus indicates whether a site is composed primarily of small or large patches of finer-scale structures. Lastly, Shannon's evenness index describes how similar the proportions of different classes are across a site (Table 3) (McGarigal and Marks 1995). We computed all heterogeneity indices using the *terra* (Hijmans et al., 2023) and *landscapemetrics* (Hesselbarth et al., 2019) packages in R (R Core Team, 2023). We used an 8-neighbor rule for defining patches of classes and computed site-level indices (i.e., across patches of all structure class types).

To assess differences in heterogeneity indices between reference and control sites, we first compared the distributions of each index (aggregation index, interspersion-juxtaposition index, area-weighted mean patch size, and Shannon's evenness index) using boxplots and violin plots. Next, we tested for multivariate differences (i.e., across all heterogeneity indices) between the reference and control sites. We used PERMANOVA to test for significant differences in the centroids of heterogeneity indices and used PERMDISP to test for significant differences in dispersion, using an α of 0.05 for both statistical tests. We first scaled

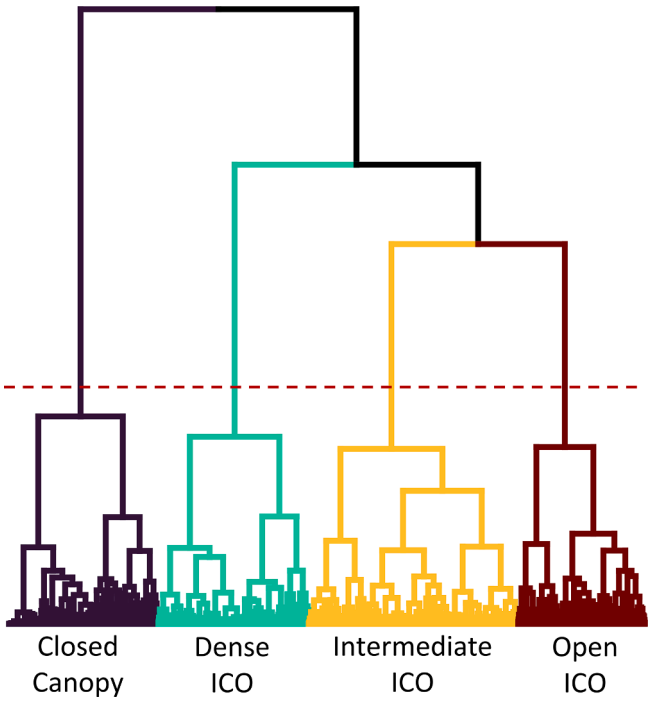

Fig. 3. Dendrogram illustrating the hierarchical clustering analysis applied to the five ICO metrics, with the horizontal line depicting the cut in the dendrogram defining four distinct structure classes (see Fig. 4). ICO refers to fine-scale spatial patterns of individual tree approximate objects (TAOs), clumps of TAOs, and open space.

each heterogeneity index by its range, then produced a Euclidean distance matrix from the scaled heterogeneity indices. We used the *adonis2* function from the *vegan* package (Oksanen et al., 2022) to run PERMANOVA and used the *betadisper* function from the *vegan* package and the base *aov* function to run PERMDISP in R (R Core Team, 2023). Lastly, we visualized differences in centroid and dispersion between reference and control sites using the first two axes of a Principal Coordinates Analysis derived from the input heterogeneity indices.

3. Results

3.1. Neighborhood-level structures

Our hierarchical clustering analysis produced a distinct set of four structure classes representing neighborhood-level (~1-ha) ICO patterns characteristic of the reference and control sites. Cutting the dendrogram at four classes was most appropriate for our dataset, as further splitting or grouping would have produced less distinct classes (Fig. 3). We provide distributions of ALS-derived tree clump and opening metrics across all pixels within reference and control sites in Appendix Fig. A3; however, we focus our results and discussion on the derived neighborhood-level structure classes since structure classes 1) are easier to interpret from a management perspective and 2) represent the metrics that were scaled up to quantify site- and among-site structural patterns.

Distributions of ICO metrics comprising each structure class and visualizations of a representative sample from each class are shown in Fig. 4. We assigned names to each structure class based on interpretations of the resultant metric distributions. The "closed canopy" class was characterized by mean 64.0% canopy area of large clumps and <15.0% mean canopy area of single TAOs and 2–4 and 5–9 TAO clumps. On the other hand, the dense, intermediate, and open ICO structure classes were all composed of >35% mean canopy/pixel area of at least one key ICO structure metric (i.e., single TAOs, 2–4 TAO clumps, or 5–9 TAO clumps). These ICO-dominated structure classes were distinguished, however, based on the relative proportion of constituent ICO metrics. The "dense ICO" class was dominated by 5–9 TAO clumps (mean 37.5% canopy area); "intermediate ICO" was dominated by 2–4 TAO clumps (mean 63.5% canopy area); and "open ICO" was dominated by open space (mean 63.3% pixel area) and single TAOs (mean 81.9% canopy area). The first and second row in Fig. 4 provide top-down visualizations of the horizontal spatial structures in each class, showing the decreasing canopy cover and more distinguished ICO structures moving from closed canopy (left) to open ICO structures (right). In Fig. 5 we provide photographs taken within representative patches (>4 contiguous 90-m pixels) of each structure class within Yosemite National Park during summer of 2022.

Comparing the mean and variance of the proportions of neighborhood-level structure classes indicated key differences between reference and control sites (Fig. 6). Reference sites on average were characterized by 29.6% open ICO structures, 39.5% intermediate ICO structures, and only 9.9% closed canopy structures. In contrast, control sites on average were composed of 48.2% closed canopy structures, 20.1% intermediate ICO structures, and only 9.8% open ICO structures. Both site types had approximately 21% dense ICO structures (Fig. 6).

3.2. Site-level spatial patterns

Comparisons of site-level heterogeneity indices indicated a more heterogeneous spatial arrangement of finer-scale structure classes in reference sites compared to controls (Fig. 7). References sites exhibited lower aggregation index, higher interspersion-juxtaposition index, smaller area-weighted mean patch size, and higher Shannon's evenness index (median AI = 33.5; median IJI = 87.1; median AWMPS = 22.3; median SHEI = 0.91) relative to controls (median AI = 41.5; median IJI = 85.2; median AWMPS = 37.2; median SHEI = 0.86). (Fig. 7A). Our multivariate comparisons (i.e., using PERMANOVA to compare all input heterogeneity indices between reference and control sites) indicated a significant difference in the centroid of heterogeneity indices between site types ($\alpha < 0.05$), suggesting that reference sites exhibited greater site-level heterogeneity (Fig. 7A/B).

3.3. Among-site variability

Comparisons of among-site variability and dispersion between reference and control sites indicated that, across the Sierra Nevada YPMC zone, sites with ongoing fire-suppression (i.e., control sites) were more variable in terms of their site-level heterogeneity indices. In contrast, reference sites were more consistently heterogeneous (i.e., lower variability in heterogeneity indices) across the Sierra Nevada YPMC zone. Standard deviations of each heterogeneity index were higher in control sites (standard deviation AI = 13.2; standard deviation IJI = 14.1; standard deviation AWMPS = 92.7; standard deviation SHEI = 0.18) compared to reference sites (standard deviation AI = 3.97; standard deviation IJI = 9.42; standard deviation AWMPS = 18.6; standard deviation SHEI = 0.06) (Fig. 7A). Additionally, we observed significantly higher multivariate dispersion of heterogeneity indices in control sites compared to reference sites (Fig. 7B).

4. Discussion

Our analyses provide key insights about the effects of a contemporary, frequent, and low-intensity fire regime on multi-scale forest structural patterns, and how these structures compare against typical fire-suppressed forests in the Sierra Nevada YPMC zone. Frequent and low-intensity fires produced distinct horizontal spatial patterns at the neighborhood-level in reference sites, with structures characterized primarily by individual TAOs, small clumps of TAOs, and high proportions of open space (Figs. 5 and 6). In contrast, fire-suppressed control sites were dominated primarily by closed canopy structures at the neighborhood-level, with only moderate proportions of dense and

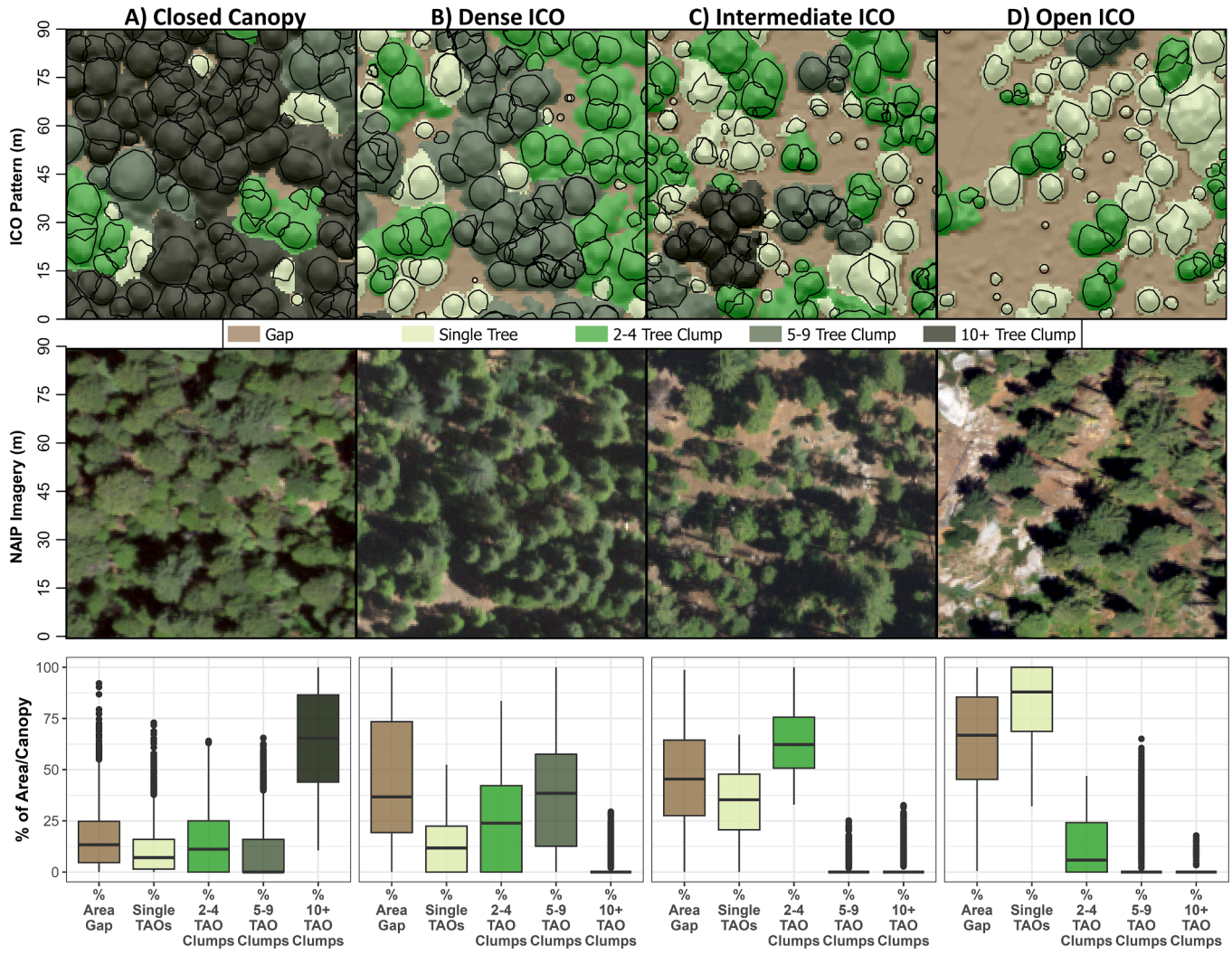

Fig. 4. Visualizations and metrics for representative samples of the four structure classes. Top row shows top-down visualization of TAO clump and opening patterns within 90x90-m (~1-ha) pixels; middle row shows top-down visualization of 0.6-m resolution National Agricultural Imagery Program (NAIP) true color images; and bottom row shows distributions of input structure metrics that define each structure class (% area for area gap metric and % canopy for all other metrics). ICO refers to fine-scale spatial patterns of individual tree approximate objects (TAOs), clumps of TAOs, and open space.

intermediate ICO structures. We observed more heterogeneous spatial arrangements of neighborhood-level structure classes within reference sites compared to controls, based on low aggregation of pixels, high interspersion of patch types, small patch sizes, and high evenness of patch types (Fig. 7). Furthermore, we found that site-level heterogeneity indices consistently fell within a relatively small range of variation *among* reference sites, while controls exhibited higher among-site variance (Fig. 7). This consistency in site-level heterogeneity among reference sites suggests a coarse-scale stabilizing effect of contemporary frequent-fire regimes, where fire as an active process ultimately leads to greater consistency of spatial patterns across broad, ecosystem scales. The multi-scale structural patterns observed in reference sites indicate improved resilience to future disturbances and climate change and will likely support other key ecosystem services; therefore, these structures can be used to help inform management efforts across the Sierra Nevada.

4.1. Neighborhood-level structures (~1 ha)

Across our reference and control sites, we observed four ecologically and statistically distinct structure classes – closed canopy, dense ICO, intermediate ICO, and open ICO. The closed canopy structure class was characteristic of fire-suppressed forests, in which key components of the ICO pattern, including individual TAOs, small clumps of TAOs, and open space, were absent. This condition is common in fire-suppressed forests due to infilling of more shade-tolerant species which increases continuity of surface, ladder, and canopy fuels (Collins et al., 2011; Lydersen et al., 2013). The three ICO structure classes (dense ICO, intermediate ICO, and open ICO), however, were characterized by higher proportions of open space, individual TAOs, and small clumps of TAOs, which represent the key horizontal structural components that define frequent-fire forests (Larson and Churchill 2012; Lydersen et al., 2013).

Our results provide evidence that the reintroduction of a frequent, low-intensity fire regime in previously fire-suppressed forests has begun to reestablish neighborhood-level ICO patterns that are similar to pre-Euro-American colonization (Larson and Churchill 2012; Churchill et al., 2013; Lydersen et al., 2013; Safford and Stevens 2017). Low-intensity fires can produce open space, single TAOs, and small clumps of TAOs by iteratively disaggregating larger contiguous clumps of TAOs, like those found in our fire-suppressed control sites (Kane et al., 2013; Kane et al., 2019; Ritter et al., 2020). Ultimately, this "breaking up" of larger clumps likely led to the formation and dominance of intermediate and open ICO structure classes in our reference sites. Importantly, our findings of mostly individual TAOs and small clumps of TAOs in fire-intact forests are consistent with past studies that analyzed TAO

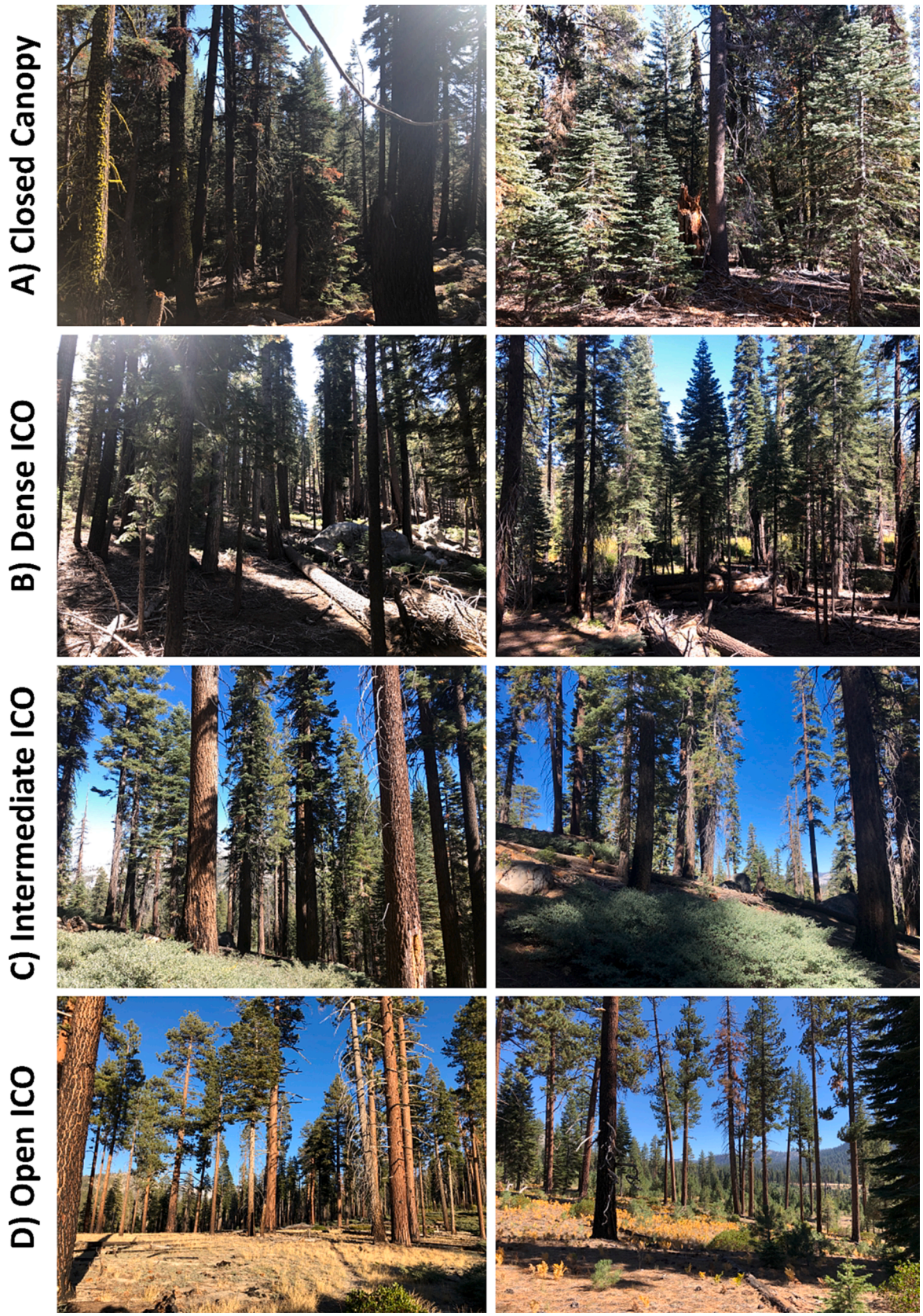

Fig. 5. Photos taken within representative patches (>4 continugous 90-m pixels) of each forest structure class during summer of 2022 site visits in Yosemite National Park. ICO refers to fine-scale spatial patterns of individual tree approximate objects (TAOs), clumps of TAOs, and open space. Photo credit Caden Chamberlain.

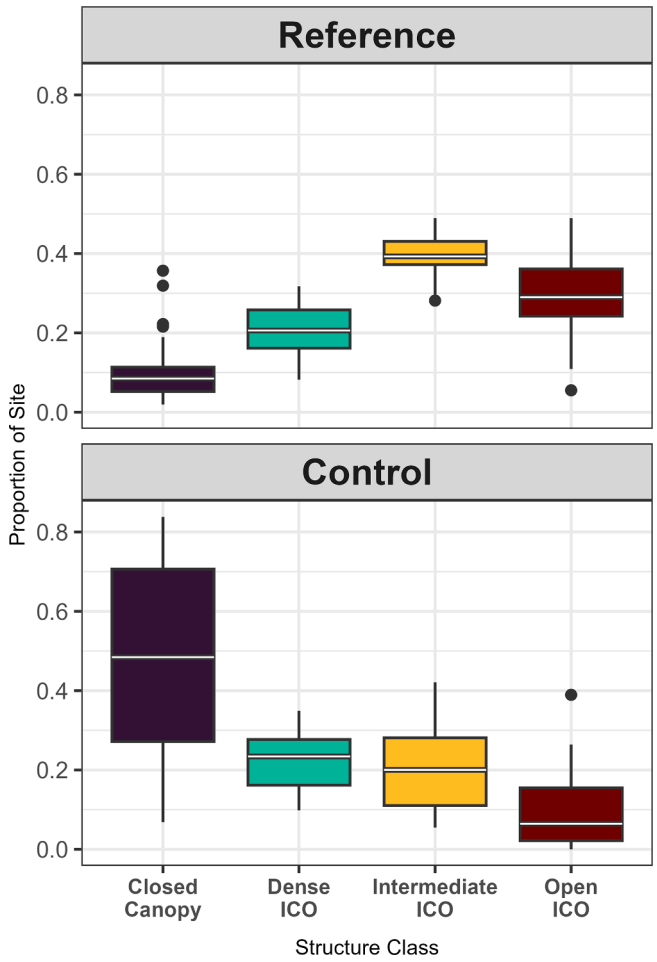

Fig. 6. Distributions of structure class proportions between reference (top) and control (bottom) sites. Each data point represents the proportion of a given structure class for a single site. Reference sites are dominated by open and intermediate ICO classes with lower proportions of dense ICO and closed canopy classes. Control sites dominated by closed canopy and to a lesser extent dense ICO structure classes, and lower portions of intermediate and open ICO classes. ICO refers to fine-scale spatial patterns of individual tree approximate objects (TAOs), clumps of TAOs, and open space.

spatial patterns in contemporary reference sites (Jeronimo et al., 2019; Wiggins et al., 2019). Additionally, despite the dominance of intermediate and open ICO structure classes, we note that reference sites on average were composed of 9.9% of the closed canopy structure class which was characterized by large TAO clumps and <10% area gap. These patches of denser canopy structures in reference sites, likely concentrated in valleys and areas with higher productivity (Collins et al., 2016; Jeronimo et al., 2019; Ng et al., 2020), contribute to other important ecosystem services like wildlife habitat and biodiversity (Meyer et al., 2007a; Stephens et al., 2016b; Kramer et al., 2021; Stephens et al., 2021; Steel et al., 2022).

Our results suggest that the fine-scale ICO structures produced from first-entry low- and moderate-severity fires can remain relatively stable through the occurrence of subsequent fires. Kane et al. (2019) found that first-entry low- and moderate-severity fires exhibited structures dominated by individual TAOs and 2–4 TAO clumps. Across our reference sites, which experienced *multiple* low- and moderate-severity fires, we found high proportions of individual TAOs and 2–4 TAO clumps, suggesting that the fine-scale ICO patterns produced during first-entry burns (Kane et al., 2019) persisted through multiple fire events. Hankin and Anderson (2022) found stability in tree density and ladder fuel density through multiple low- and moderate-severity fires in the Sierra Nevada; our results provide additional insight about the stability of TAO spatial patterns, which represent a critical structural component in frequent-fire systems (Larson and Churchill 2012; Lydersen et al., 2013). However, it should be noted that without pre- and post-fire data for each fire, we were unable to know for certain if the neighborhood-level structures were either present prior to fire or were produced by first or subsequent burns.

While we found that fire-suppressed control sites were indeed dominated by closed-canopy structures, we also observed that nearly half of the area of control sites was characterized by dense and intermediate ICO structures (24% and 19%, respectively). This highlights that the signal of edaphic-driven structures has persisted, to some extent, through fire suppression – where edaphic conditions can produce persistent canopy gaps that do not support tree regeneration or formation of large tree clumps (North et al., 2004; Meyer et al., 2007b; Fry et al., 2014). It is also likely that other non-fire disturbances contributed to the formation of dense and intermediate ICO structures in controls. While we used LCMS data to partially account for the effects of other disturbances, it is likely that this dataset did not capture all isolated drought, insect, and pathogen induced mortality (Housman et al., 2022), which could theoretically produce dense or intermediate ICO structures (Steel et al., 2022). Importantly, these lower density ICO structures observed in control sites could potentially provide anchors for future resilience-focused treatments in the Sierra Nevada (Larson et al., 2013).

4.2. *Site-level structures (~100–1,000 ha)*

Within reference sites (~100–1,000 ha), our results suggest that frequent and low-intensity fires produced a disaggregated and interspersed arrangement of mostly small (<50-ha) patches, primarily representing intermediate and open ICO structure classes. We assert that greater interspersion of neighborhood-level structures, smaller patch sizes, and higher evenness of patch types (compared to controls) is indicative of increased *heterogeneity* at the within-site level in reference sites (see Fig. 7C). This site-level heterogeneity demonstrates the capacity of a restored, low-intensity, and frequent fire regime to create variable structures within previously fire-suppressed forests, like those found in our control sites.

The spatial variability and stochasticity of recent fire intensity and resultant severity was likely a driving force of the site-level heterogeneity observed in our reference sites. Stochasticity and variability in fire behavior is driven by variability in fire weather, fuels, topography, and moisture gradients at fine- to moderate-spatial scales (Parsons et al., 2017; Sullivan 2017; Jeronimo et al., 2020). As fires burn across a site they interact with the biophysical environment and the legacies of recent disturbances (Kane et al., 2015; Harvey et al., 2016; Hessburg et al., 2019). For example, higher productivity sites may have higher fuel moisture, which could reduce fire intensity and result in reduced overstory mortality and therefore patches of denser ICO structures (Lydersen et al., 2013; Jeronimo et al., 2019; Ng et al., 2020). In contrast, exposed topographic positions may burn at higher intensities and result in more intermediate and open ICO structures (Lydersen et al., 2013; Jeronimo et al., 2019; Ng et al., 2020). Subsequent fires then interact with this variability in structure and fuels to further increase heterogeneity across the landscape (Kane et al., 2015; Koontz et al., 2020), as evidenced by the highly interspersed, disaggregated, and small patch sizes of forest structure classes observed within reference sites in our study.

4.3. *Among-site-level structures (~10,000-100,000 ha)*

We observed lower *among*-site (~10,000–100,000 ha) variance and dispersion in heterogeneity indices (i.e., aggregation index, interspersion-juxtaposition index, area-weighted mean patch size, and Shannon's evenness index) for reference sites compared to control sites. This suggests a possible coarse-scale stabilizing effect of a frequent, low-

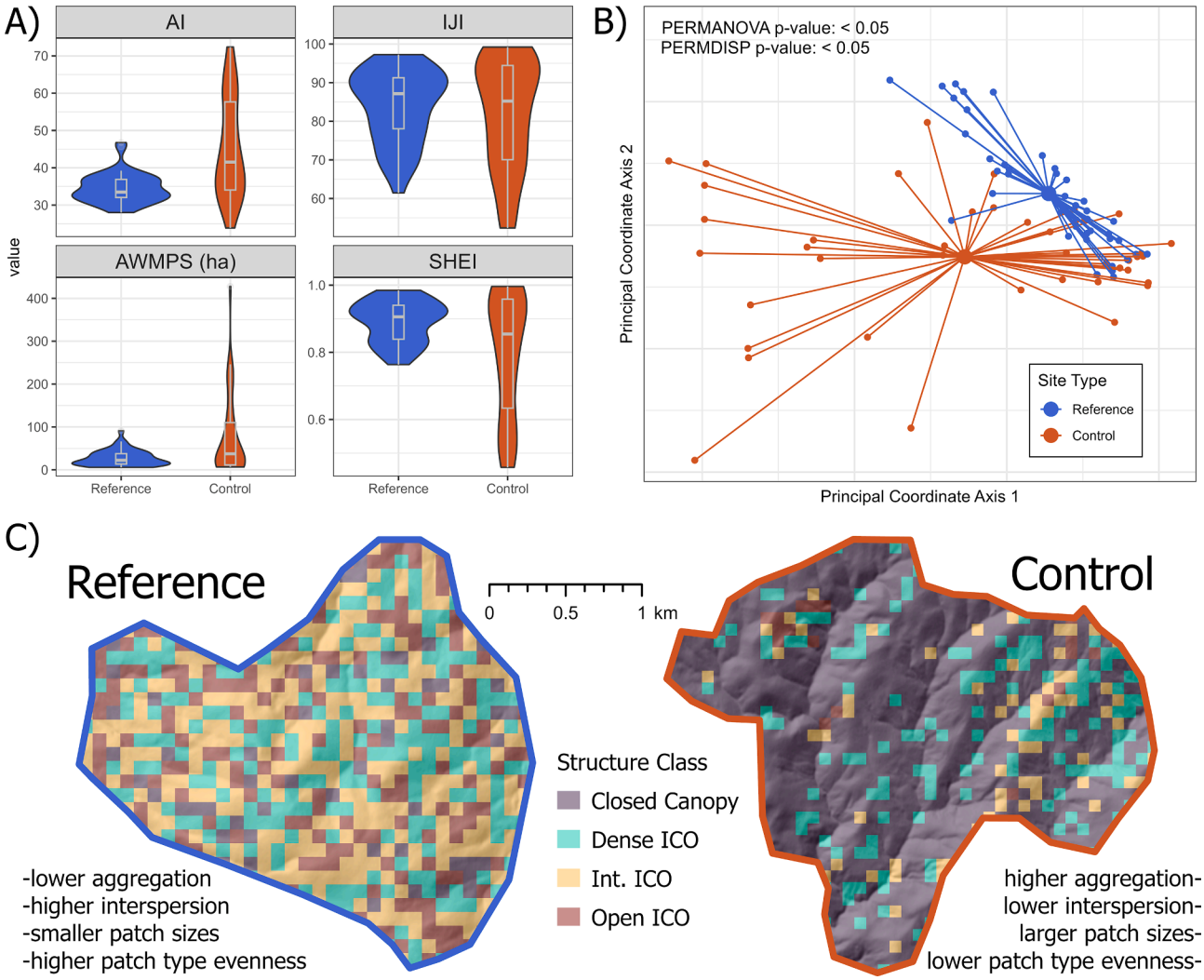

Fig. 7. Comparisons of the distributions of heterogeneity indices between the reference (blue) and control (orange) sites (panel A). Heterogeneity indices were calculated using all four structure classes. Indices include aggregation index (AI), interspersion-juxtaposition index (IJI), area-weighted mean patch size (AWMPS), and Shannon's evenness index (SHEI). Principal Coordinates Analysis (PCoA) ordination derived from the input site-level heterogeneity indices comparing the multivariate centroid and dispersion between reference and control sites (panel B). PCoA Axis 1 was most strongly correlated with SHEI and AI. PCoA Axis 2 was most strongly correlated with AWMPS and IJI. Difference in centroids between sites tested using PERMANOVA and differences in dispersion between sites tested using PERMDISP ($\alpha = 0.05$). Visualization of representative reference (left) and control (right) sites with mapped forest structure classes showing differences in aggregation, interspersion, patch sizes, and evenness between the sites (panel C).

intensity fire regime. For example, area-weighted mean patch size ranged from 6 to 91 ha across reference sites but ranged from 7 to 427 ha across controls. Importantly, reference sites exhibited this relatively high site-level heterogeneity regardless of variability in other fire regime and biophysical drivers, such as variability in the intensity and resultant severity of past fires, past fire frequencies (2 versus 4 recent fires), topographic conditions, or productivity gradients. Therefore, we contend that a frequent and low-intensity fire regime represents a strong driver of site-level heterogeneity, producing consistent patterns across broad, ecosystem scales. This inference is strengthened by comparison to reconstructed historical frequent-fire forests in the Pacific Northwest where Churchill et al. (2013), Churchill et al. (2017), and LeFevre et al. (2020) all found similar ranges of variation in forest structure and spatial patterns across relatively disparate ecosystems (eastern Washington Cascades, southern Blue Mountains, and northeastern Washington Rockies, respectively).

We found relatively higher variance in aggregation, interspersion, patch size, and patch type evenness indices in the control sites compared to the reference sites. While other minor disturbance agents and edaphic drivers may sometimes result in moderate or high levels of heterogeneity in the absence of fire, our results suggest that these drivers do not consistently produce heterogeneous structures across the region, especially not to the same extent as a restored, frequent, and low-intensity fire regime. Nonetheless, it is important to note that nearly half of control sites *were* characterized by heterogeneity indices similar to reference sites, indicating a potential boon for restoration efforts in the Sierra Nevada. Fire suppressed forests with edaphic or other disturbance-driven heterogeneity may exhibit improved resilience to future disturbances and climate change due to their structural variability (Hessburg et al., 2019). In these sites, perhaps only minimal restoration treatments or the use of unplanned ignitions to support resource objectives (i.e., wildland fire use) will be required to improve resilience (Weatherspoon and Skinner, 1995; North et al., 2021; Ziegler et al., 2021).

4.4. Management implications

4.4.1. Resilience and ecosystem services

We posit that the neighborhood-level ICO structure classes dominating the reference sites, as well as the increased site-level

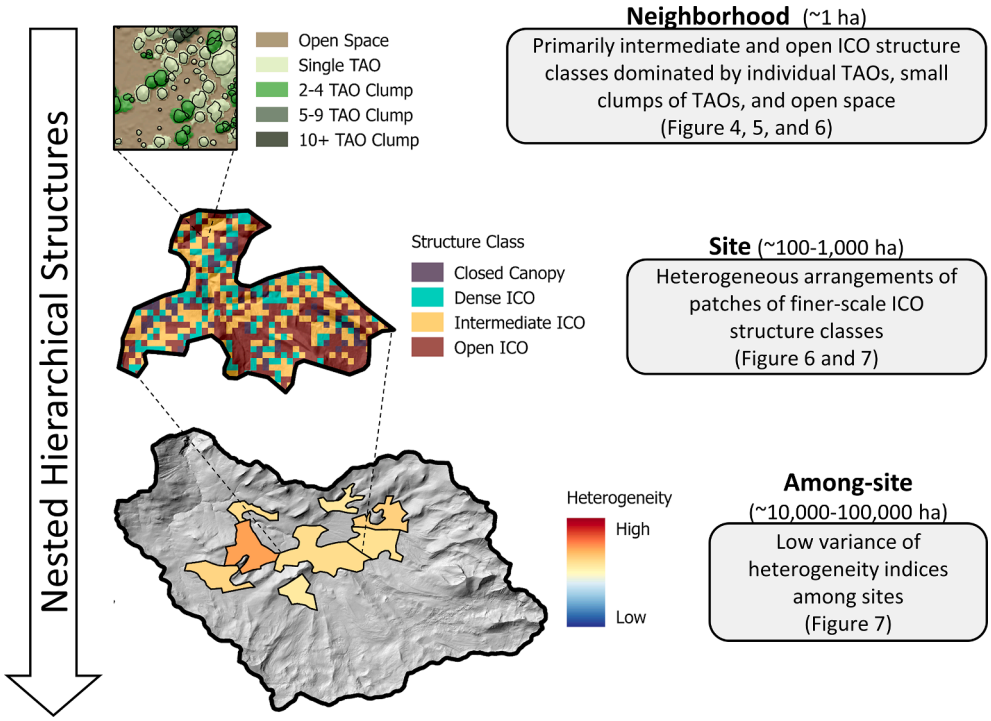

Fig. 8. A nested hierarchical set of structural patterns observed in reference sites characterized by a frequent, low-intensity fire regime. At the neighborhood-level (~1 ha), structures are dominated by intermediate and open ICO structures consisting primarily of individual TAOs, small clumps of TAOs, and high proportions of open space. At the site-level (~100–1,000 ha), patches of ICO structure classes are arranged heterogeneously, with small patch sizes and high interspersion of patch types. Among-sites (~10,000–100,000 ha) there is low variance of heterogeneity indices; all sites consistently exhibit high interspersion of patches, small patch sizes, and high evenness of patch types. ICO refers to fine-scale spatial patterns of individual tree approximate objects (TAOs), clumps of TAOs, and open space.

heterogeneity of these ICO structures, will confer greater resilience in the face of future fires, droughts, and climate change (Moritz et al., 2010; Hessburg et al., 2015; Hessburg et al., 2019; Newman et al., 2019; Francis et al., 2023). We define resilience as the capacity of YPMC forests to maintain a stable range of structure, composition, and functional integrity through periodic disturbances like fire, drought, and insect outbreaks (Walker et al., 2004; North et al., 2022). Heterogeneity at the site-level in reference sites also suggests improvements to other important ecosystem services like wildlife habitat, biodiversity, and ecosystem capacity for climate adaptation (Dudney et al., 2018; Kramer et al., 2021; Stephens et al., 2021). As such, the multi-scale structural patterns observed in reference sites can be used by managers as diagnostics when designing and implementing restoration treatments or when evaluating the effects of recent disturbances on resilience and other ecosystem services.

At the neighborhood-level, high proportions of open space in the intermediate and open ICO structure classes suggests reduced and discontinuous surface fuels, which will likely minimize crown fire initiation and subsequent high severity fire (Agee and Skinner 2005; Ziegler et al., 2021). Additionally, during future fires, convective cooling around single TAOs and 2–4 TAO clumps may increase overstory tree survival and thus reduce burn severity (Pimont et al., 2009; Ziegler et al., 2017; Ritter et al., 2020). Higher proportions of sun-exposed gaps and bare mineral soil will also increase the probability of post-fire regeneration and recovery, especially for more fire-resistant and shade-intolerant species like ponderosa pine and Jeffrey pine (Zald et al., 2008; Bigelow et al., 2011). Additionally, lower tree densities will lead to reduced competition for water and light which may increase individual tree health and allow trees to better resist second-order post-fire mortality (Jeronimo et al., 2020). More vigorous trees may also exhibit improved defense mechanisms against future drought and insect disturbances and increased survival under projected warmer and drier climates (Hood et al., 2015; Koontz et al., 2021; Furniss et al., 2022).

The site-level heterogeneity observed in our reference sites also suggests improved resilience to future disturbances and climate change. First, more heterogeneous patch structures will promote variability in future fire behavior across these sites (Hessburg et al., 2019). This variability in fire behavior could theoretically reduce the likelihood of large contiguous high-severity patches (Koontz et al., 2020; Francis et al., 2023) which are known to negatively impact non-serotinous conifer re-establishment and thus post-fire recovery (Coop et al., 2020; Jeronimo et al., 2020; Steel et al., 2021). Site-level heterogeneity also indicates a mosaic of microclimates with varying temperature and moisture gradients, which may provide distinct microsites of cooler and wetter conditions that promote regeneration success of key conifer species under a warmer and drier climate (De Frenne et al., 2013; Davis et al., 2019). Some research also indicates that more heterogeneous structures across sites and landscapes can impede the spread of bark beetles or other pathogens, which may ensure that these disturbances remain at endemic levels under increasingly unfavorable climatic conditions (Fettig et al., 2007; North 2012; Pile et al., 2019).

Heterogeneous structures at the neighborhood- and site-level in reference sites also suggest improvements to other important ecosystem services like wildlife habitat, biodiversity, and climate adaptive capacity. Variability in structures across sites, ranging from closed canopy to open ICO structure classes, provide a range of habitat components that support nesting and foraging for species like the California spotted owl (White et al., 2013; Stephens et al., 2016b; Kramer et al., 2021; Steel et al., 2022). Increased heterogeneity at multiple scales will also increase floral and faunal biodiversity (Tingley et al., 2016; Kelly et al., 2017; Stephens et al., 2021). For example, patches of dense ICO structures likely have higher proportions of shade-tolerant species like white and red fir while patches of intermediate and open ICO structures are likely dominated by shade-intolerant species like Jeffrey pine and sugar pine (Zald et al., 2008; Bigelow et al., 2011; Stephens et al., 2021). This variability in vegetation structures in reference sites may also promote

increased adaptive capacity under climate change (Gunderson 2000; Dudney et al., 2018). Heterogeneity across different spatial scales promotes redundancy of resilience mechanisms, which supports a wider range of vegetation responses to shifting climates and disturbance regimes across space and time (Peterson et al., 1998; Dobrowski, 2011; Hannah et al., 2014).

4.4.2. Hierarchical structures to guide ecosystem management

We quantified a nested, hierarchical set of forest structure metrics in restored frequent-fire reference sites of the Sierra Nevada YPMC zone, which provides a scalable set of observations that managers can use to guide management efforts in the region. Past work has described hierarchical arrangements of structural patterns in both historical and contemporary frequent-fire forests (e.g., Larson and Churchill 2012; Reynolds et al., 2013; Churchill et al., 2017; Hessburg et al., 2019). However, our study is unique in using lidar data to explicitly quantify and describe structures at these nested hierarchical scales.

We suggest conceptualizing ecosystem structures of frequent-fire forests as a hierarchy of structural components – beginning with trees and open space and scaling these components up to the neighborhood-, site-, and among-site-level (Fig. 8). At the finest scale, individual trees, small clumps of mostly 2–4 trees, and open space represent the primary structural components, with only moderate representation of larger tree clumps. At the neighborhood-level (~1 ha), individual trees and small clumps of trees are arranged within a matrix of open space. At the site-level (~100–1,000 ha), these neighborhood structures can be grouped into small patches (mostly < 50 ha in size) of similar structures and arranged in heterogeneous and intermixed patterns across the site. Arrangements of structure class patches can be guided by topographic position and productivity gradients (i.e., dense ICO and small patches of closed canopy structures in more productive sites and open and intermediate ICO structures in less productive sites) (Collins et al., 2016; Jeronimo et al., 2019; Ng et al., 2020). Lastly, at the among-site-level, for example across a watershed or Forest Service district, all sites should fall within a narrow range of site-level heterogeneity indices (i.e., patch sizes ranging from ~ 5–90 ha, or aggregation indices ranging from ~28–46) and should be representative of a diversity of neighborhood-level structures (Fig. 8).

An important outcome of our work is that our within-site analysis fills a critical information gap between fine- and broad-scale spatial patterns in a way that is applicable to operational forest landscape restoration. Frameworks have been proposed and applied for both landscape-scale prioritization and planning (Manley et al., 2020; Larson et al., 2022) and within-stand treatment guidelines (North et al., 2009; Churchill et al., 2013; Knapp et al., 2017) but linking these two scales has been a challenge in practice. Our analyses suggest that a relatively simple set of fine-scale structural components – proportions of individual trees, clumps of trees, and open space – can be scaled up to characterize reference site structures at the neighborhood-, within-site, and among-site-levels. These structural patterns thus provide guidelines for landscape restoration that 1) capture the hierarchical and cross-scale structure of ecosystems and 2) can be operationalized at each spatial scale by aggregating metrics from finer-scales (Hessburg et al., 2015).

4.5. Study limitations and future research

We acknowledge several limitations to the present study that should be considered by managers and ecologists when interpreting our results. These limitations present opportunities for future research in active-fire landscapes of the Sierra Nevada.

Structural conditions observed in the reference sites only represent a snapshot in space and time and may continue to change as additional fires burn through these sites and structures are influenced by both direct and indirect effects of climate change. While recent research suggests that continued occurrence of low-intensity fires in these sites is unlikely to substantially alter structural patterns beyond their current conditions (Hankin and Anderson 2022), other work suggests that long-term shifts in climate and its influence on future fire intensities may indeed lead to considerable shifts in structures in these sites (Crompton et al., 2022). As such, we recommend that managers use the reference conditions defined in our analyses as a baseline for designing and evaluating treatments in the 21st century in combination with adaptive management frameworks that update management strategies to account for uncertainty and changing conditions (Gunderson 2000; Stephens et al., 2010; Millar et al., 2007). Additionally, managers could consider designing treatments based on reference conditions from future, rather than current, climate conditions, as described in Churchill et al. (2013). Further research that explicitly tests the resilience of these reference sites based on the capacity of structures to persist and recover under future disturbances and climate change is also needed (e.g., Lydersen et al., 2014; Hankin and Anderson 2022).

We focused our analyses on horizontal forest structures since these structures are known to be important mechanisms of resilience in historically frequent-fire forests and since they can more easily be aggregated to characterize coarser resolution structures (Larson and Churchill 2012). Yet, we recognize that vertical canopy arrangements are important structural features in frequent-fire systems as well (North et al., 2009; Ziegler et al., 2017). For example, reduced fuel laddering can reduce the likelihood of crown fire initiation (Agee and Skinner 2005), while within clump variability in tree heights can be a proxy for uneven aged distributions which may engender greater resilience to insect outbreaks (Restaino et al., 2019). While not explicitly evaluated in our analyses, past research suggests that the ICO patterns observed in contemporary reference sites in the Sierra Nevada are indeed characterized by reduced lower strata canopy cover and higher variability in tree heights both within and among tree clumps (Kane et al., 2014; Kane et al., 2015; North et al., 2017; Kane et al., 2019). Therefore, we expect similar patterns in the reference sites analyzed in the present study. Additional summaries of vertical structure metrics across reference sites are also provided in the associated Data in Brief paper (Chamberlain et al., 2023a, *in review*).

While ALS data enables high fidelity and extensive characterization of overstory canopy structures across reference sites, these ALS datasets also have several limitations. For example, a single tree segmented from ALS data may realistically represent multiple on-the-ground trees if the segmentation algorithm fails to separate interlocked canopies and subordinate trees, hence our use of the term 'tree approximate objects' (TAOs) (Jeronimo et al., 2018). Because of this, our metrics related to tree clumping patterns should be interpreted as broad trends. Since one TAO may represent several on-the-ground trees (especially those falling under the canopy of larger trees), we expect that our clumping metrics tend to report smaller clump sizes than would be expected from *in situ* field measurements that include lower-canopy trees (Jeronimo et al., 2018; Wiggins et al., 2019). This assertion is justified by comparing our clumping metrics against tree spatial patterns recorded in historical datasets which generally reported larger clump sizes (Lydersen et al., 2013).

We also acknowledge the inability of ALS data to characterize and quantify species composition and surface fuel conditions, which are certainly important factors that influence forest resilience (Lydersen et al., 2013; Prichard et al., 2017; Bernal et al., 2022). Based on the occurrence of multiple low-intensity fires in the contemporary reference sites, we contend that these sites are likely dominated by more fire-resistant species like ponderosa pine, Jeffrey pine, and Douglas-fir (Safford and Stevens 2017), and that surface fuel loading is reduced compared to control sites. Still, we encourage future research that explicitly maps and quantifies species and surface fuels in contemporary reference sites, especially as climate change continues to influence post-fire tree recruitment and overstory tree survivorship (Liang et al., 2017; Davis et al., 2023).

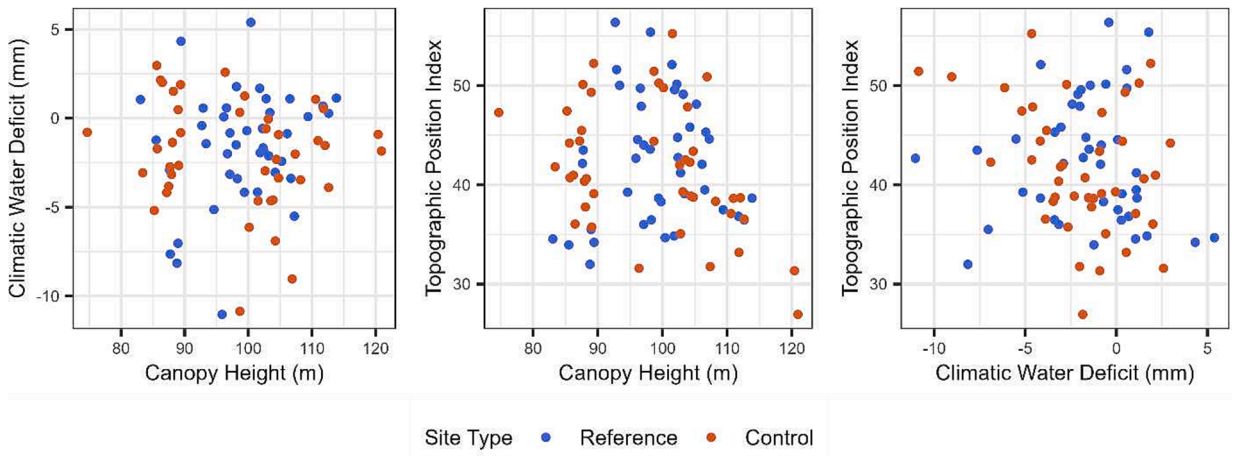

Fig. A1. Scatterplots showing mean canopy height (m) vs. climatic water deficit (mm) vs. topographic position index for reference and control sites. Canopy height represents lidar-derived 95th percentile of tree approximate object (TAO) heights.

5. Conclusion

In yellow pine and mixed-conifer (YPMC) forests of California's Sierra Nevada, more than a century of fire suppression and long-term shifts in land management practices have led to considerable changes in forest processes and structures (Collins et al., 2011; Knapp et al., 2013). In recent years, these altered conditions, coupled with climate change, have brought a new fire regime to the Sierra Nevada, characterized by larger and often more severe fires than historical conditions (Stevens et al., 2017; Williams et al., 2019; Williams et al., 2023). However, this changing fire landscape has also enabled the formation of several contemporary reference sites across the Sierra Nevada where repeated low/moderate-severity fires have occurred in recent decades, and thus a frequent, low-intensity fire regime has begun to reestablish in the modern era (Jeronimo et al., 2019; Cova et al., 2023). In this study, we analyzed forest structural patterns at multiple scales in contemporary reference sites and compared structures against typical fire-suppressed control sites to identify key structures produced by a contemporary, low-intensity, and frequent fire regime.

We observed a nested and hierarchical set of structural patterns across reference sites that indicate a stabilizing effect of a frequent, low-intensity fire regime across broad, ecosystem scales. High proportions of individual TAOs, small clumps of TAOs, and open space formed intermediate and open ICO structures at the neighborhood-level, and these structures were consistently arranged in heterogenous spatial patterns across all reference sites. In fire suppressed control sites, edaphic factors and other non-fire disturbances produced variability in structures at different spatial scales, but this structural variability was not as consistent compared to reference sites. Importantly, control sites with higher proportions of closed canopy structures and low site-level heterogeneity indices could be prioritized in regional restoration planning efforts to ensure treatment of higher-risk areas. We encourage forest and fire managers in the Sierra Nevada to use the multi-scale and hierarchical structural patterns identified in reference sites to inform and guide management across the region.

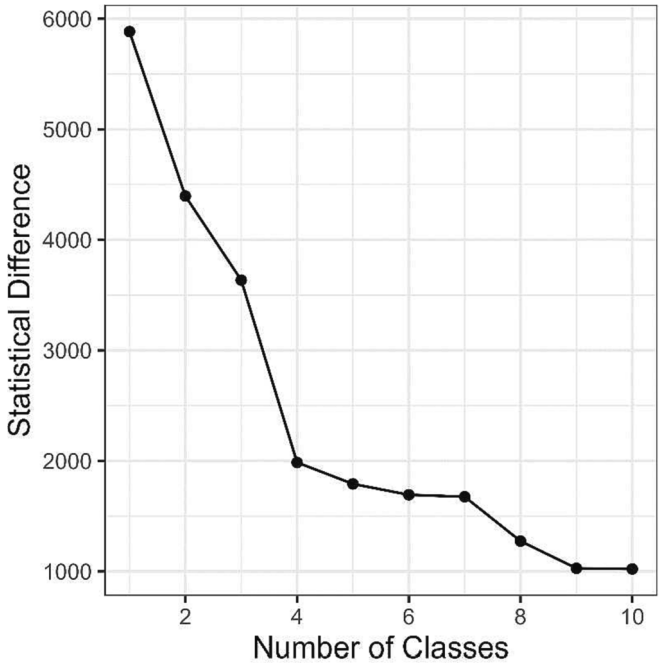

Fig. A2. Scree plot derived from the hierarchical clustering applied to the five ICO structure metrics. Four classes represent an appropriate place to cut the dendrogram as further splitting or grouping does not lead to substantial increases in statistical difference.

CRediT authorship contribution statement

Caden P. Chamberlain: Conceptualization, Methodology, Software, Formal analysis, Investigation, Writing – original draft, Visualization. **Gina R. Cova:** Conceptualization, Methodology, Software, Resources, Writing – review & editing. **C. Alina Cansler:** Conceptualization, Methodology, Supervision, Writing – review & editing. **Malcolm P. North:** Conceptualization, Methodology, Writing – review & editing, Supervision. **Marc D. Meyer:** Conceptualization, Methodology, Writing – review & editing. **Sean M.A. Jeronimo:** Conceptualization, Methodology, Writing – review & editing, Resources. **Van R. Kane:** Conceptualization, Methodology, Resources, Writing – review & editing, Supervision, Funding acquisition.

Declaration of Competing Interest

The authors declare that they have no known competing financial interests or personal relationships that could have appeared to influence the work reported in this paper.

Data availability

Contemporary reference sites and associated forest structure datasets are available on the Forest Service Research Data Archive (https://doi.

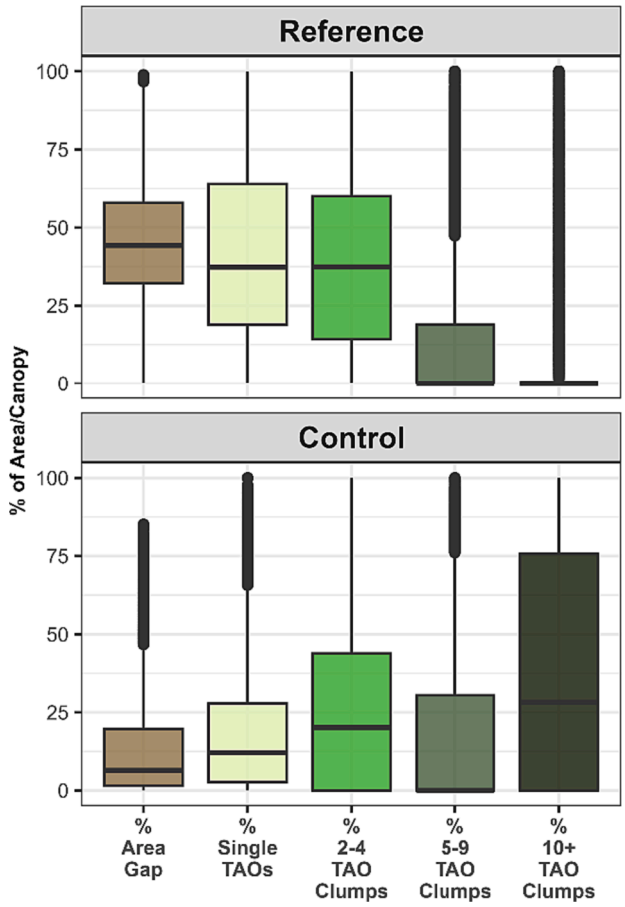

Fig. A3. Distributions of neighborhood-level (i.e., 90 m pixel) structure metrics across reference (top) and control (bottom) sites (% area for area gap metric and % canopy for all other metrics). ICO refers to fine-scale spatial patterns of individual tree approximate objects (TAOs), clumps of TAOs, and open space.

org/10.2737/RDS-2023-0027; Chamberlain et al., 2023b). Control sites, representing fire-suppressed forests, are available on the Zenodo Digital Repository (https://doi.org/10.5281/zenodo.8401035). All other data will be made available upon request.

Acknowledgements

This work was supported by 1) NASA's Future Investigators in NASA Earth and Space Science and Technology (FINESST) Earth Science Research Program grant (#80NSSC21K1588), 2) a United States Department of Agriculture (USDA) Southwest Research Station grant (#20-JV-11272138-035), and 3) a USDA Pacific Northwest Research Station grant (#20-JV-11261989-068). Additionally, we thank Jonathan Kane, Bryce Bartl-Geller, and Liz van Wagtendonk with the University of Washington for assistance with lidar data processing and interpretation.

Appendix

Appendix A. Supplementary material

Supplementary data to this article can be found online at https://doi.org/10.1016/j.foreco.2023.121478.

References

Agee, J.K., Skinner, C.N., 2005. Basic principles of forest fuel reduction treatments. For. Ecol. Manag. 211 (1), 83–96. https://doi.org/10.1016/j.foreco.2005.01.034.

Allen, I., Chhin, S., Zhang, J., 2019. Fire and forest management in montane forests of the northwestern states and California, USA. Fire 2 (2), 17. https://doi.org/10.3390/fire2020017.

Anderson, M.K., Moratto, M.J., 1996, January. Native American land-use practices and ecological impacts. In Sierra Nevada ecosystem project: final report to Congress (pp. 187-206). Davis, CA: University of California, Centers for Water and Wildland Resources Davis.

Atchley, A.L., Linn, R., Jonko, A., Hoffman, C., Hyman, J.D., Pimont, F., Sieg, C., Middleton, R.S., 2021. Effects of fuel spatial distribution on wildland fire behaviour. Int. J. Wildland Fire 30 (3), 179–189. https://doi:10.1071/WF20096.

Bernal, A.A., Stephens, S.L., Collins, B.M., Battles, J.J., 2022. Biomass stocks in California's fire-prone forests: Mismatch in ecology and policy. Environ. Res. Lett. 17 (4), 044047 https://doi.org/10.1088/1748-9326/ac576a.

Bigelow, S.W., North, M.P., Salk, C.F., 2011. Using light to predict fuels-reduction and group-selection effects on succession in Sierran mixed-conifer forest. Can. J. For. Res. 41 (10), 2051–2063. https://doi.org/10.1139/x11-120.

Bonnicksen, T.M., Stone, E.C., 1980. The giant sequoia—mixed conifer forest community characterized through pattern analysis as a mosaic of aggregations. For. Ecol. Manag. 3, 307–328. https://doi.org/10.1016/0378-1127(80)90031-6.

Carpenter, S., Walker, B., Anderies, J.M., Abel, N., 2001. From metaphor to measurement: resilience of what to what? Ecosystems 4, 765–781. https://doi.org/10.1007/s10021-001-0045-9.

Chamberlain, C.P., Cova, G.R., Cansler, C.A., Kane, J.T., Bartl-Geller, B., van Wagtendonk L., Jeronimo, S.M.A., Stine, P., North, M.P., Kane, V.R., 2023a. Sierra Nevada reference conditions: a dataset of contemporary reference sites and corresponding remote sensing-derived forest structure metrics for yellow pine and mixed-conifer forests. Data in Brief. In Review.

Chamberlain, C.P., Cova, G.R., Kane, V.R., Cansler, C.A., Bartl-Geller, B.N., Kane, J.T., Jeronimo, S.M.A., Stine, P.A., North, M.P., 2023b. Sierra Nevada contemporary reference site boundaries and corresponding remote sensing-derived canopy structure rasters. Fort Collins, CO: Forest Service Research Data Archive. https://doi.org/10.2737/RDS-2023-0027.

Churchill, D.J., Carnwath, G.C., Larson, A.J., Jeronimo, S.M.A., 2017. Historical forest structure, composition, and spatial pattern in dry conifer forests of the western Blue Mountains, Oregon (Gen. Tech. Rep. PNW-GTR-956). US Department of Agriculture, Forest Service, Pacific Northwest Research Station. https://doi.org/10.2737/PNW-GTR-956.

Churchill, D.J., Larson, A.J., Dahlgreen, M.C., Franklin, J.F., Hessburg, P.F., Lutz, J.A., 2013. Restoring forest resilience: From reference spatial patterns to silvicultural prescriptions and monitoring. For. Ecol. Manag. 291, 442–457. https://doi.org/10.1016/j.foreco.2012.11.007.

Collins, B.M., Miller, J.D., Thode, A.E., Kelly, M., van Wagtendonk, J.W., Stephens, S.L., 2009. Interactions among wildland fires in a long-established Sierra Nevada natural fire area. Ecosystems 12 (1), 114–128. https://doi.org/10.1007/s10021-008-9211-7.

Collins, B.M., Everett, R.G., Stephens, S.L., 2011. Impacts of fire exclusion and recent managed fire on forest structure in old growth Sierra Nevada mixed-conifer forests. Ecosphere 2 (4), 51. https://doi.org/10.1890/ES11-00026.1.

Collins, B.M., Lydersen, J.M., Everett, R.G., Fry, D.L., Stephens, S.L., 2015. Novel characterization of landscape-level variability in historical vegetation structure. Ecol. Appl. 25 (5), 1167–1174. https://doi.org/10.1890/14-1797.1.

Collins, B.M., Lydersen, J.M., Fry, D.L., Wilkin, K., Moody, T., Stephens, S.L., 2016. Variability in vegetation and surface fuels across mixed-conifer-dominated landscapes with over 40 years of natural fire. For. Ecol. Manag. 381, 74–83. https://doi.org/10.1016/j.foreco.2016.09.010.

Coop, J.D., Parks, S.A., Stevens-Rumann, C.S., Crausbay, S.D., Higuera, P.E., Hurteau, M. D., Tepley, A., Whitman, E., Assal, T., Collins, B.M., Davis, K.T., Dobrowski, S., Falk, D.A., Fornwalt, P.J., Fulé, P.Z., Harvey, B.J., Kane, V.R., Littlefield, C.E., Margolis, E.Q., North, M., Parisien, M.-A., Prichard, S., Rodman, K.C., 2020. Wildfire-driven forest conversion in western North American landscapes. Bioscience 70 (8), 659–673.

Cova, G., Kane, V.R., Prichard, S., North, M., Cansler, C.A., 2023. The outsized role of California's largest wildfires in changing forest burn patterns and coarsening ecosystem scale. For. Ecol. Manag. 528, 120620 https://doi.org/10.1016/j.foreco.2022.120620.

Crompton, O.V., Boisrame, G.F.S., Rakhmatulina, E., Stephens, S.L., Thompson, S.E., 2022. Fire return intervals explain different vegetation cover responses to wildfire restoration in two Sierra Nevada basins. For. Ecol. Manag. 521, 120429. https://doi.org/10.1016/j.foreco.2022.120429.

Cushman, S.A., McGarigal, K., Neel, M.C., 2008. Parsimony in landscape metrics: Strength, universality, and consistency. Ecol. Ind. 8 (5), 691–703. https://doi.org/10.1016/j.ecolind.2007.12.002.

Cutler, D.R., Edwards, J.T.C., Beard, K.H., Cutler, A., Hess, K.T., Gibson, J., Lawler, J.J., 2007. Random Forests for classification in ecology. Ecology 88 (11), 2783–2792. https://doi.org/10.1890/07-0539.1.

Davis, K.T., Robles, M.D., Kemp, K.B., Higuera, P.E., Chapman, T., Metlen, K.L., Peeler, J. L., Rodman, K.C., Woolley, T., Addington, R.N., Buma, B.J., Cansler, C.A., Case, M.J., Collins, B.M., Coop, J.D., Dobrowski, S.Z., Gill, N.S., Haffey, C., Harris, L.B., Harvey, B.J., Haugo, R.D., Hurteau, M.D., Kulakowski, D., Littlefield, C.E., McCauley, L.A., Povak, N., Shive, K.L., Smith, E., Stevens, J.T., Stevens-Rumann, C. S., Taylor, A.H., Tepley, A.J., Young, D.J.N., Andrus, R.A., Battaglia, M.A., Berkey, J. K., Busby, S.U., Carlson, A.R., Chambers, M.E., Dodson, E.K., Donato, D.C., Downing, W.M., Fornwalt, P.J., Halofsky, J.S., Hoffman, A., Holz, A., Iniguez, J.M.,

Krawchuk, M.A., Kreider, M.R., Larson, A.J., Meigs, G.W., Roccaforte, J.P., Rother, M.T., Safford, H., Schaedel, M., Sibold, J.S., Singleton, M.P., Turner, M.G., Urza, A.K., Clark-Wolf, K.D., Yocom, L., Fontaine, J.B., Campbell, J.L., 2023. Reduced fire severity offers near-term buffer to climate-driven declines in conifer resilience across the western United States. Proc. Natl. Acad. Sci. 120 (11), e2208120120 https://doi.org/10.1073/pnas.2208120120.

Davis, F.W., Synes, N.W., Fricker, G.A., McCullough, I.M., Serra-Diaz, J.M., Franklin, J., Flint, A.L., 2019. LiDAR-derived topography and forest structure predict fine-scale variation in daily surface temperatures in oak savanna and conifer forest landscapes. Agric. For. Meteorol. 269–270, 192–202. https://doi.org/10.1016/j.agrformet.2019.02.015.

De Frenne, P., Rodríguez-Sánchez, F., Coomes, D.A., Baeten, L., Verstraeten, G., Vellend, M., Bernhardt-Römermann, M., Brown, C.D., Brunet, J., Cornelis, J., Decocq, G.M., Dierschke, H., Eriksson, O., Gilliam, F.S., Hédl, R., Heinken, T., Hermy, M., Hommel, P., Jenkins, M.A., Kelly, D.L., Kirby, K.J., Mitchell, F.J.G., Naaf, T., Newman, M., Peterken, G., Petřík, P., Schultz, J., Sonnier, G., Van Calster, H., Waller, D.M., Walther, G.-R., White, P.S., Woods, K.D., Wulf, M., Graae, B.J., Verheyen, K., 2013. Microclimate moderates plant responses to macroclimate warming. Proc. Natl. Acad. Sci. 110 (46), 18561–18565.

DeRose, R.J., Long, J.N., 2014. Resistance and resilience: A conceptual framework for silviculture. For. Sci. 60, 1205–1212. https://doi.org/10.5849/forsci.13-507.

Dobrowski, S.Z., 2011. A climatic basis for microrefugia: the influence of terrain on climate. Glob. Chang. Biol. 17, 1022–1035. https://doi.org/10.1111/j.1365-2486.2010.02263.x.

Dudney, J., Hobbs, R.J., Heilmayr, R., Battles, J.J., Suding, K.N., 2018. Navigating novelty and risk in resilience management. Trends Ecol. Evol. 33, 863–873. https://doi.org/10.1016/j.tree.2018.08.012.

EPA Ecoregions. Environmental Protection Agency Level IV Ecoregions. [accessed March 2023]. https://www.epa.gov/eco-research/ecoregion-download-files-state-region-9#pane-04.

ESRI World Imagery. Environmental Systems Research Institute World Imagery. [accessed September 2021]. https://www.arcgis.com/home/item.html?id=c03a526d94704bfb839445e80de95495.

Falk, D.A., Watts, A.C., Thode, A.E., 2019. Scaling ecological resilience. Front. Ecol. Evol. 7 https://doi.org/10.3389/fevo.2019.00275.

Falk, D.A., van Mantgem, P.J., Keeley, J.E., Gregg, R.M., Guiterman, C.H., Tepley, A.J., Young, D.J.N., Marshall, L.A., 2022. Mechanisms of forest resilience. For. Ecol. Manag. 512, 120129 https://doi.org/10.1016/j.foreco.2022.120129.

Fettig, C.J., Klepzig, K.D., Billings, R.F., Munson, A.S., Nebeker, T.E., Negrón, J.F., Nowak, J.T., 2007. The effectiveness of vegetation management practices for prevention and control of bark beetle infestations in coniferous forests of the western and southern United States. For. Ecol. Manag. 238 (1), 24–53. https://doi.org/10.1016/j.foreco.2006.10.011.

Flint, L.E., Flint, A.L., Stern, M.A., 2021. The basin characterization model—A regional water balance software package. Reston, VA: U.S. Geological Survey Techniques and Methods Report No.: 6-H1. [accessed 2022 Dec 8]. http://pubs.er.usgs.gov/publication/tm6H1.

Forest Management Task Force, 2021. California's Wildfire and Forest Resilience Action Plan. https://wildfiretaskforce.org/action-plan/.

Francis, E.J., Pourmohammadi, P., Steel, Z.L., Collins, B.M., Hurteau, M.D., 2023. Proportion of forest area burned at high-severity increases with increasing forest cover and connectivity in western US watersheds. Landsc. Ecol. 38 (10), 2501–2518.

FRAP Fire Perimeters. California Department of Forestry and Fire Protection's Fire and Resource Assessment Program (FRAP). [accessed July 2021]. https://frap.fire.ca.gov/mapping/gis-data/.

Fry, D.L., Stephens, S.L., Collins, B.M., North, M.P., Franco-Vizcaíno, E., Gill, S.J., Jose, S., 2014. Contrasting spatial patterns in active-fire and fire-suppressed Mediterranean climate old-growth mixed conifer forests. PLoS One 9 (2), e88985. https://doi.org/10.1371/journal.pone.0088985.

Furniss, T.J., Das, A.J., van Mantgem, P.J., Stephenson, N.L., Lutz, J.A., 2022. Crowding, climate, and the case for social distancing among trees. Ecol. Appl. 32 (2), e2507.

FVEG, 2015. California Department of Forestry and Fire Protection's Fire and Resource Assessment Program (FRAP). [accessed July 2021]. https://map.dfg.ca.gov/metadata/ds1327.html.

Gatziolis, D., Andersen, H.E., 2008. A guide to LIDAR data acquisition and processing for the forests of the Pacific Northwest (Gen. Tech. Rep. PNW-GTR-768). US Department of Agriculture, Forest Service, Pacific Northwest Research Station. https://www.fs.usda.gov/treesearch/pubs/30652.

Gotelli, N.J., Ellison, A.M., 2018. A Primer of Ecological Statistics, second ed. Sinauer Associates, Inc., Oxford University Press, Sunderland, MA.

Greiner, S.M., Grimm, K.E., Waltz, A.E.M., 2020. Managing for resilience? Examining management implications of resilience in southwestern National Forests. J. For. 118 (4), 433–443.

Gunderson, L.H., 2000. Ecological resilience—in theory and application. Annu. Rev. Ecol. Evol. Syst. 31 (1), 425–439. https://doi.org/10.1146/annurev.ecolsys.31.1.425.

Hagmann, R.K., Hessburg, P.F., Prichard, S.J., Povak, N.A., Brown, P.M., Fulé, P.Z., Keane, R.E., Knapp, E.E., Lydersen, J.M., Metlen, K.L., Reilly, M.J., Sánchez Meador, A.J., Stephens, S.L., Stevens, J.T., Taylor, A.H., Yocom, L.L., Battaglia, M.A., Churchill, D.J., Daniels, L.D., Falk, D.A., Henson, P., Johnston, J.D., Krawchuk, M.A., Levine, C.R., Meigs, G.W., Merschel, A.G., North, M.P., Safford, H.D., Swetnam, T. W., Waltz, A.E.M., 2021. Evidence for widespread changes in the structure, composition, and fire regimes of western North American forests. Ecol. Appl. 31 (8) https://doi.org/10.1002/eap.2431.

Hankin, L.E., Anderson, C.T., 2022. Second-entry burns reduce mid-canopy fuels and create resilient forest structure in Yosemite National Park, California. Forests 13 (9), 1512. https://doi.org/10.3390/f13091512.

Hannah, L., Flint, L., Syphard, A.D., Moritz, M.A., Buckley, L.B., McCullough, I.M., 2014. Fine-grain modeling of species' response to climate change: holdouts, stepping-stones, and microrefugia. Trends Ecol. Evol. 29, 390–397. https://doi.org/10.1016/j.tree.2014.04.006.

Harvey, B.J., Donato, D.C., Turner, M.G., 2016. Burn me twice, shame on who? Interactions between successive forest fires across a temperate mountain region. Ecology 97 (9), 2272–2282. https://doi.org/10.1002/ecy.1439.

He, H.S., DeZonia, B.E., Mladenoff, D.J., 2000. An aggregation index (AI) to quantify spatial patterns of landscapes. Landsc. Ecol. 15 (7), 591–601. https://doi.org/10.1023/A:1008102521322.

Hessburg, P.F., Smith, B.G., Salter, R.B., Ottmar, R.D., Alvarado, E., 2000. Recent changes (1930s–1990s) in spatial patterns of interior northwest forests. USA. for. Ecol. Manag. 136 (1), 53–83. https://doi.org/10.1016/S0378-1127(99)00263-7.

Hessburg, P.F., Churchill, D.J., Larson, A.J., Haugo, R.D., Miller, C., Spies, T.A., North, M.P., Povak, N.A., Belote, R.T., Singleton, P.H., Gaines, W.L., Keane, R.E., Aplet, G.H., Stephens, S.L., Morgan, P., Bisson, P.A., Rieman, B.E., Salter, R.B., Reeves, G.H., 2015. Restoring fire-prone Inland Pacific landscapes: seven core principles. Landsc. Ecol. 30 (10), 1805–1835.

Hessburg, P.F., Miller, C.L., Parks, S.A., Povak, N.A., Taylor, A.H., Higuera, P.E., Prichard, S.J., North, M.P., Collins, B.M., Hurteau, M.D., Larson, A.J., Allen, C.D., Stephens, S.L., Rivera-Huerta, H., Stevens-Rumann, C.S., Daniels, L.D., Gedalof, Ze'ev, Gray, R.W., Kane, V.R., Churchill, D.J., Hagmann, R.K., Spies, T.A., Cansler, C.A., Belote, R.T., Veblen, T.T., Battaglia, M.A., Hoffman, C., Skinner, C.N., Safford, H.D., Salter, R.B., 2019. Climate, environment, and disturbance history govern resilience of western North American forests. Front. Ecol. Evol. 7 https://doi.org/10.3389/fevo.2019.00239.

Hesselbarth, M.H., Sciaini, M., With, K.A., Wiegand, K., Nowosad, J., 2019. landscapemetrics: an open-source R tool to calculate landscape metrics. R package version 1.5.5. Ecography 42, 1648–1657. https://doi.org/10.1111/ecog.04617.

Hijmans, R.J., Bivand, R., Pebesma, E., Sumner, M., 2023. terra: Spatial Data Analysis. R package version 1.6.7. https://rspatial.org/index.html.

Hood, S., Sala, A., Heyerdahl, E.K., Boutin, M., 2015. Low-severity fire increases tree defense against bark beetle attacks. Ecology 96 (7), 1846–1855. https://doi.org/10.1890/14-0487.1.

Housman, I., Campbell, L., Heyer, J., Goetz, W., Finco, M., Pugh, N., 2022. US Forest Service Landscape Change Monitoring System Methods. Version 2021.7.

Jeronimo, S.M.A., Kane, V.R., Churchill, D.J., McGaughey, R.J., Franklin, J.F., 2018. Applying LiDAR individual tree detection to management of structurally diverse forest landscapes. J. For. 116, 336–346. https://doi.org/10.1093/jofore/fvy023.

Jeronimo, S.M.A., Kane, V.R., Churchill, D.J., Lutz, J.A., North, M.P., Asner, G.P., Franklin, J.F., 2019. Forest structure and pattern vary by climate and landform across active-fire landscapes in the montane Sierra Nevada. For. Ecol. Manag. 437, 70–86. https://doi.org/10.1016/j.foreco.2019.01.033.

Jeronimo, S.M.A., Lutz, J.A., Kane, V.R., Larson, A.J., Franklin, J.F., 2020. Burn weather and three-dimensional fuel structure determine post-fire tree mortality. Landsc. Ecol. 35, 859–878. https://doi.org/10.1007/s10980-020-00983-0.

Kane, V.R., Lutz, J.A., Roberts, S.L., Smith, D.F., McGaughey, R.J., Povak, N.A., Brooks, M.L., 2013. Landscape-scale effects of fire severity on mixed-conifer and red fir forest structure in Yosemite National Park. For. Ecol. Manag. 287, 17–31. https://doi.org/10.1016/j.foreco.2012.08.044.

Kane, V.R., North, M.P., Lutz, J.A., Churchill, D.J., Roberts, S.L., Smith, D.F., McGaughey, R.J., Kane, J.T., Brooks, M.L., 2014. Assessing fire effects on forest spatial structure using a fusion of Landsat and airborne LiDAR data in Yosemite National Park. Remote Sens. Environ. 151, 89–101. https://doi.org/10.1016/j.rse.2013.07.041.

Kane, V.R., Lutz, J.A., Cansler, C.A., Povak, N.A., Churchill, D.J., Smith, D.F., Kane, J.T., North, M.P., 2015. Water balance and topography predict fire and forest structure patterns. For. Ecol. Manag. 338, 1–13. https://doi.org/10.1016/j.foreco.2014.10.038.

Kane, V.R., Bartl-Geller, B.N., North, M.P., Kane, J.T., Lydersen, J.M., Jeronimo, S.M.A., Collins, B.M., Monika Moskal, L., 2019. First-entry wildfires can create opening and tree clump patterns characteristic of resilient forests. For. Ecol. Manag. 454, 117659 https://doi.org/10.1016/j.foreco.2019.117659.

Keane, R.E., Hessburg, P.F., Landres, P.B., Swanson, F.J., 2009. The use of historical range and variability (HRV) in landscape management. For. Ecol. Manag. 258, 1025–1037. https://doi.org/10.1016/j.foreco.2009.05.035.

Knapp, E.E., Skinner, C.N., North, M.P., Estes, B.L., 2013. Long-term overstory and understory change following logging and fire exclusion in a Sierra Nevada mixed-conifer forest. For. Ecol. Manag. 310, 903–914. https://doi.org/10.1016/j.foreco.2013.09.041.

Kelly, L.T., Brotons, L., McCarthy, M.A., 2017. Putting pyrodiversity to work for animal conservation. Conserv. Biol. 31 (4), 952–955. https://www.jstor.org/stable/44331550.

Knapp, E.E., Lydersen, J.M., North, M.P., Collins, B.M., 2017. Efficacy of variable density thinning and prescribed fire for restoring forest heterogeneity to mixed-conifer forest in the central Sierra Nevada. CA. for. Ecol. Manag. 406, 228–241. https://doi.org/10.1016/j.foreco.2017.08.028.

Knight, C.A., Tompkins, R.E., Wang, J.A., York, R., Goulden, M.L., Battles, J.J., 2022. Accurate tracking of forest activity key to multi-jurisdictional management goals: A case study in California. J. Environ. Manage. 302, 114083 https://doi.org/10.1016/j.jenvman.2021.114083.

Koontz, M.J., North, M.P., Werner, C.M., Fick, S.E., Latimer, A.M., Swenson, N., 2020. Local forest structure variability increases resilience to wildfire in dry western U.S. coniferous forests. Ecol. Lett. 23 (3), 483–494.
Koontz, M.J., Latimer, A.M., Mortenson, L.A., Fettig, C.J., North, M.P., 2021. Cross-scale interaction of host tree size and climatic water deficit governs bark beetle-induced tree mortality. Nat. Commun. 12 (1), 129. https://doi.org/10.1038/s41467-020-20455-y.
Kramer, H.A., Jones, G.M., Kane, V.R., Bartl-Geller, B., Kane, J.T., Whitmore, S.A., Berigan, W.J., Dotters, B.P., Roberts, K.N., Sawyer, S.C., Keane, J.J., North, M.P., GutiÉrrez, R.J., Peery, M.Z., 2021. Elevational gradients strongly mediate habitat selection patterns in a nocturnal predator. Ecosphere 12, e03500.
Larson, A.J., Belote, R.T., Cansler, C.A., Parks, S.A., Dietz, M.S., 2013. Latent resilience in ponderosa pine forest: effects of resumed frequent fire. Ecol. Appl. 23 (6), 1243–1249. https://doi.org/10.1890/13-0066.1.
Larson, A.J., Churchill, D., 2012. Tree spatial patterns in fire-frequent forests of western North America, including mechanisms of pattern formation and implications for designing fuel reduction and restoration treatments. For. Ecol. Manag. 267, 74–92. https://doi.org/10.1016/j.foreco.2011.11.038.
Larson, A.J., Jeronimo, S.M.A., Hessburg, P.F., Lutz, J.A., Povak, N.A., Cansler, C.A., Kane, V.R., Churchill, D.J., 2022. Tamm Review: Ecological principles to guide post-fire forest landscape management in the Inland Pacific and Northern Rocky Mountain regions. For. Ecol. Manag. 504, 119680 https://doi.org/10.1016/j.foreco.2021.119680.
LeFevre, M.E., Churchill, D.J., Larson, A.J., Jeronimo, S.M.A., Bass, J., Franklin, J.F., Kane, V.R., 2020. Evaluating restoration treatment effectiveness through a comparison of residual composition, structure, and spatial pattern with historical reference sites. For. Sci. 66 (5), 578–588. https://doi.org/10.1093/forsci/fxaa014.
Liang, S., Hurteau, M.D., Westerling, A.L., 2017. Response of Sierra Nevada forests to projected climate–wildfire interactions. Glob. Chang. Biol. 23 (5), 2016–2030. https://doi.org/10.1111/gcb.13544.
Liaw, A., Wiener, M., 2002. Classification and regression by randomForest. R package version 4.7-1.1. https://CRAN.R-project.org/doc/Rnews/.
Loudermilk, E.L., O'Brien, J.J., Goodrick, S.L., Linn, R.R., Skowronski, N.S., Hiers, J.K., 2022. Vegetation's influence on fire behavior goes beyond just being fuel. Fire Ecol. 18 (1), 9. https://doi.org/10.1186/s42408-022-00132-9.
Lydersen, J.M., North, M.P., 2012. Topographic variation in active-fire forest structure under current climate conditions. Ecosyst. 15, 1134–1146. https://doi.org/10.1007/s10021-012-9573-8.
Lydersen, J.M., North, M.P., Knapp, E.E., Collins, B.M., 2013. Quantifying spatial patterns of tree groups and gaps in mixed-conifer forests: Reference conditions and long-term changes following fire suppression and logging. For. Ecol. Manag. 304, 370–382. https://doi.org/10.1016/j.foreco.2013.05.023.
Lydersen, J.M., North, M.P., Collins, B.M., 2014. Severity of an uncharacteristically large wildfire, the Rim Fire, in forests with relatively restored frequent fire regimes. For. Ecol. Manag. 328, 326–334. https://doi.org/10.1016/j.foreco.2014.06.005.
Manley, P., Wilson, K., Povak, N., 2020. Framework for promoting socio-ecological resilience across forested landscapes in the Sierra Nevada. Sierra Nevada Conservancy.
Massip, N., 2020. The 1964 Wilderness Act, from "wilderness idea" to governmental oversight and protection of wilderness. Miranda 20. https://doi.org/10.4000/miranda.26787.
McGarigal, K., Marks, B.J., 1995. FRAGSTATS: spatial pattern analysis program for quantifying landscape structure (Gen. Tech. Rep. PNW-GTR-351). US Department of Agriculture, Forest Service, Pacific Northwest Research Station. https://www.fs.usda.gov/treesearch/pubs/3064.
McGaughey, R.J., 2020. FUSION/LDV: Software for LIDAR Data Analysis and Visualization: Version 4.00. USDA Forest Service Pacific Northwest Research Station, Seattle, WA. http://forsys.cfr.washington.edu/FUSION/fusion_overview.html.
Meigs, G.W., Case, M.J., Churchill, D.J., Hersey, C.M., Jeronimo, S.M.A., Smith, L.A.C., Thom, D., 2023. Drought, wildfire and forest transformation: Characterizing trailing edge forests in the eastern Cascade Range, Washington, USA. Forestry 96 (3), 340–354.
Meyer, M.D., Kelt, D., North, M.P., 2007a. Microhabit associations of northern flying squirrels in burned and thinned stands of the Sierra Nevada. Am. Midl. Nat. 157, 202–211.
Meyer, M.D., North, M.P., Gray, A.N., Zald, H.S.J., 2007b. Influence of soil thickness on stand characteristics in a Sierra Nevada mixed-conifer forest. Plant and Soil 294 (1), 113–123. https://doi.org/10.1007/s11104-007-9235-3.
Millar, C.I., Stephenson, N.L., Stephens, S.L., 2007. Climate change and forests of the future: managing in the face of uncertainty. Ecol. Appl. 17 (8), 2145–2151.
Miller, J.D., Thode, A.E., 2007. Quantifying burn severity in a heterogeneous landscape with a relative version of the delta Normalized Burn Ratio (dNBR). Remote Sens. Environ. 109 (1), 66–80. https://doi.org/10.1016/j.rse.2006.12.006.
Moritz, M.A., Hessburg, P.F. and Povak, N.A., 2010. Native fire regimes and landscape resilience. The Landscape Ecology of Fire (pp. 51-86). Dordrecht: Springer Netherlands.
Newman, E.A., Kennedy, M.C., Falk, D.A., McKenzie, D., 2019. Scaling and complexity in landscape ecology. Front. Ecol. Evol. 7, 293.
Ng, J., North, M.P., Arditti, A.J., Cooper, M.R., Lutz, J.A., 2020. Topographic variation in tree group and gap structure in Sierra Nevada mixed-conifer forests with active fire regimes. For. Ecol. Manag. 472, 118220 https://doi.org/10.1016/j.foreco.2020.118220.
NHDPlusV2. Environmental Protection Agency National Hydrogrpahy Dataset Plus. [accessed July 2021]. https://www.epa.gov/waterdata/nhdplus-national-data.
North, M., Chen, J., Oakley, B., Song, B., Rudnicki, M., Gray, A., Innes, J., 2004. Forest stand structure and pattern of old-growth western hemlock/Douglas-fir and mixed-conifer forests. For. Sci. 50 (3), 299–311. https://doi.org/10.1093/forestscience/50.3.299.
North, M., Collins, B.M., Safford, H., Stephenson, N.L., 2016. Montane forests. Montane forests. In: Harold, M., Erika, Z. (Eds.), Ecosystems of California. University of California Press, Berkeley, CA, pp. 553–577.
North, M., Stine, P., O'Hara, K., Zielinski, W., Stephens, S., 2009. An ecosystem management strategy for Sierran mixed-conifer forests (Gen. Tech. Rep. PSW-GTR-220). US Department of Agriculture, Forest Service, Pacific Southwest Research Station. http://www.fs.usda.gov/treesearch/pubs/32916.
North, M.P., York, R.A., Collins, B.M., Hurteau, M.D., Jones, G.M., Knapp, E.E., Kobziar, L., McCann, H., Meyer, M.D., Stephens, S.L., et al., 2021. Pyrosilviculture needed for landscape resilience of dry western United States forests. J. For. 119(5), 520–544. https://doi.org 10.1093/jofore/fvab026.
North, M.P., Kane, J.T., Kane, V.R., Asner, G.P., Berigan, W., Churchill, D.J., Conway, S., Gutiérrez, R.J., Jeronimo, S.M.A., Keane, J., Koltunov, A., Mark, T., Moskal, L.M., Munton, T., Peery, Z., Ramirez, C., Sollmann, R., White, A.M., Whitmore, S., 2017. Cover of tall trees best predicts California spotted owl habitat. For. Ecol. Manag. 405, 166–178. https://doi.org/10.1016/j.foreco.2017.09.019.
North, M.P., Tompkins, R.E., Bernal, A.A., Collins, B.M., Stephens, S.L., York, R.A., 2022. Operational resilience in western US frequent-fire forests. For. Ecol. Manag. 507, 120004 https://doi.org/10.1016/j.foreco.2021.120004.
North, M., 2012. Managing Sierra Nevada forests. Structure (Gen. Tech. Rep. PSW-GTR-237). US Department of Agriculture, Forest Service, Pacific Southwest Research Station. https://www.fs.usda.gov/treesearch/pubs/40254.
Oksanen, J., Simpson, G., Blanchet, F., Kindt, R., Legendre, P., Minchin, P., O'Hara, R., Solymos, P., Stevens, M., Szoecs, E., et al., 2022. vegan: Community Ecology Package. R package version 2.6-4. https://CRAN.R-project.org/package=vegan.
Parks, S.A., Holsinger, L.M., Koontz, M.J., Collins, L., Whitman, E., Parisien, M.A., Loehman, R.A., Barnes, J.L., Bourdon, J.F., Boucher, J., et al., 2019. Giving ecological meaning to satellite-derived fire severity metrics across North American forests. Remote Sens. 11 (14), 1735.
Parsons, R.A., Linn, R.R., Pimont, F., Hoffman, C., Sauer, J., Winterkamp, J., Sieg, C.H., Jolly, W.M., 2017. Numerical investigation of aggregated fuel spatial pattern impacts on fire behavior. Land 6 (2), 43. https://doi.org/10.3390/land6020043.
Pawlikowski, N.C., Coppoletta, M., Knapp, E., Taylor, A.H., 2019. Spatial dynamics of tree group and gap structure in an old-growth ponderosa pine-California black oak forest burned by repeated wildfires. For. Ecol. Manag. 434, 289–302. https://doi.org/10.1016/j.foreco.2018.12.016.
Peterson, G., Allen, C.R., Holling, C.S., 1998. Ecological resilience, biodiversity, and scale. Ecosystems 1, 6–18. https://doi.org/10.1007/s100219900002.
Pile, L.S., Meyer, M.D., Rojas, R., Roe, O., Smith, M.T., 2019. Drought impacts and compounding mortality on forest trees in the southern Sierra Nevada. Forests 10 (3), 237. https://doi.org/10.3390/f10030237.
Pimont, F., Dupuy, J.L., Caraglio, Y., Morvan, D., 2009. Effect of vegetation heterogeneity on radiative transfer in forest fires. Int. J. Wildland Fire 18 (5), 536–553. https://doi.org/10.1071/WF07115.
Prichard, S.J., Stevens-Rumann, C.S., Hessburg, P.F., 2017. Tamm Review: Shifting global fire regimes: Lessons from reburns and research needs. For. Ecol. Manag. 396, 217–233. https://doi.org/10.1016/j.foreco.2017.03.035.
R Core Team, 2023. R version 4.2.2. R: a language and environment for statistical computing. R Foundation for Statistical Computing, Vienna, Austria. www.R-project.org.
Restaino, C., Young, D.J.N., Estes, B., Gross, S., Wuenschel, A., Meyer, M., Safford, H., 2019. Forest structure and climate mediate drought-induced tree mortality in forests of the Sierra Nevada, USA. Ecol. Appl. 29 (4), e01902.
Reynolds, R.T., Sánchez Meador, A.J., Youtz, J.A., Nicolet, T., Matonis, M.S., Jackson, P.L., DeLorenzo, D.G., Graves, A.D., 2013. Restoring composition and structure in Southwestern frequent-fire forests: A science-based framework for improving ecosystem resiliency (Gen. Tech. Rep. RMRS-GTR-310). US Department of Agriculture, Forest Service, Pacific Southwest Research Station. http://www.fs.usda.gov/treesearch/pubs/44885.
Richardson, J.J., Moskal, L.M., 2011. Strengths and limitations of assessing forest density and spatial configuration with aerial LiDAR. Remote Sens. Environ. 115 (10), 2640–2651. https://doi.org/10.1016/j.rse.2011.05.020.
Ritter, S.M., Hoffman, C.M., Battaglia, M.A., Stevens-Rumann, C.S., Mell, W.E., 2020. Fine-scale fire patterns mediate forest structure in frequent-fire ecosystems. Ecosphere 11 (7).
Safford, H.D., Stevens, J.T., 2017. Natural range of variation for yellow pine and mixed-conifer forests in the Sierra Nevada, southern Cascades, and Modoc and Inyo National Forests, California, USA. Forests (Gen. Tech. Rep. PSW-GTR-256). US Department of Agriculture, Forest Service, Pacific Southwest Research Station. http://www.fs.usda.gov/treesearch/pubs/55393.
Safford, H.D., Paulson, A.K., Steel, Z.L., Young, D.J.N., Wayman, R.B., 2020. The 2020 California fire season: A year like no other, a return to the past or a harbinger of the future? Glob. Ecol. Biogeogr. 31 (10), 2005–2025. https://doi.org/10.1111/geb.13498.
Schulze, S.S., Fischer, E.C., Hamideh, S., Mahmoud, H., 2020. Wildfire impacts on schools and hospitals following the 2018 California Camp Fire. Nat. Hazards. 104(1), 901–925. https://doi.org/10.1007/s11069-020-04197-0.
Singleton, M.P., Thode, A.E., Sánchez Meador, A.J., Iniguez, J.M., 2019. Increasing trends in high-severity fire in the southwestern USA from 1984 to 2015. For. Ecol. Manag. 433, 709–719. https://doi.org/10.1016/j.foreco.2018.11.039.
Steel, Z.L., Safford, H.D., Viers, J.H., 2015. The fire frequency-severity relationship and the legacy of fire suppression in California forests. Ecosphere 6 (1), 1–23.
Steel, Z.L., Foster, D., Coppoletta, M., Lydersen, J.M., Stephens, S.L., Paudel, A., Markwith, S.H., Merriam, K., Collins, B.M., 2021. Ecological resilience and

vegetation transition in the face of two successive large wildfires. J. Ecol. 109 (9), 3340–3355. https://doi.org/10.1111/1365-2745.13764.
Steel, Z.L., Jones, G.M., Collins, B.M., Green, R., Koltunov, A., Purcell, K.L., Sawyer, S.C., Slaton, M.R., Stephens, S.L., Stine, P., et al., 2022. Mega-disturbances cause rapid decline of mature conifer forest habitat in California. Ecol. Appl. 33 (2), e2763.
Stephens, S.L., Battaglia, M.A., Churchill, D.J., Collins, B.M., Coppoletta, M., Hoffman, C. M., Lydersen, J.M., North, M.P., Parsons, R.A., Ritter, S.M., et al., 2021. Forest restoration and fuels reduction: convergent or divergent? Bioscience 71 (1), 85–101. https://doi.org/10.1093/biosci/biaa134.
Stephens, S.L., Millar, C.I., Collins, B.M., 2010. Operational approaches to managing forests of the future in Mediterranean regions within a context of changing climates. Environ. Res. Lett. 5(2), 024003. https://doi.org/10.1088/1748-9326/5/2/024003.
Stephens, S.L., Collins, B.M., Biber, E., Fulé, P.Z., 2016a. U.S. federal fire and forest policy: emphasizing resilience in dry forests. Ecosphere. 7(11), e01584. https://doi.org/10.1002/ecs2.1584.
Stephens, S.L., Lydersen, J.M., Collins, B.M., Fry, D.L., Meyer, M.D., 2015. Historical and current landscape-scale ponderosa pine and mixed conifer forest structure in the Southern Sierra Nevada. Ecosphere 6 (5), art79.
Stephens, S.L., Miller, J.D., Collins, B.M., North, M.P., Keane, J.J., Roberts, S.L., 2016b. Wildfire impacts on California spotted owl nesting habitat in the Sierra Nevada. Ecosphere 7 (11), e01478.
Stevens, J.T., Collins, B.M., Miller, J.D., North, M.P., Stephens, S.L., 2017. Changing spatial patterns of stand-replacing fire in California conifer forests. For. Ecol. Manag. 406, 28–36. https://doi.org/10.1016/j.foreco.2017.08.051.
Sullivan, A.L., 2017. Inside the Inferno: Fundamental processes of wildland fire behavior. Curr. for. Rep. 3 (2), 132–149. https://doi.org/10.1007/s40725-017-0057-0.
Taylor, A.H., Trouet, V., Skinner, C.N., Stephens, S., 2016. Socioecological transitions trigger fire regime shifts and modulate fire–climate interactions in the Sierra Nevada, USA, 1600–2015 CE. Proc. Natl. Acad. Sci. 113 (48), 13684–13689. https://doi.org/10.1073/pnas.1609775113.
Tingley, M.W., Ruiz-Gutiérrez, V., Wilkerson, R.L., Howell, C.A., Siegel, R.B., 2016. Pyrodiversity promotes avian diversity over the decade following forest fire. P. Roy. Soc B-Biol. Sci. 283 (1840), 20161703. https://doi.org/10.1098/rspb.2016.1703.
Turner, M.G., Romme, W.H., 1994. Landscape dynamics in crown fire ecosystems. Landsc. Ecol. 9 (1), 59–77. https://doi.org/10.1007/BF00135079.
USDA FACTS. United States Department of Agriculture Forest Service Activity Tracking System. [accessed July 2021]. https://data.fs.usda.gov/geodata/edw/datasets.php.
van Mantgem, P.J., Stephenson, N.L., Knapp, E., Battles, J., Keeley, J.E., 2011. Long-term effects of prescribed fire on mixed conifer forest structure in the Sierra Nevada. California. for. Ecol. Manag. 261, 989–994. https://doi.org/10.1016/j.foreco.2010.12.013.
van Wagtendonk, W.J., 2007. The history and evolution of wildland fire use. Fire Ecol. 3 (2), 3–17. https://doi.org/10.4996/fireecology.0302003.
van Wagtendonk, J.W., Sugihara, N.G., Stephens, S.L., Thode, A.E., Shaffer, K.E., Fites-Kaufman, J., 2018. Fire in California's ecosystems, Second edition. University of California Press, Oakland, California.
Vincent, L., Soille, P., 1991. Watersheds in digital spaces: An efficient algorithm based on immersion simulations. IEEE Trans. Pattern Anal. Mach. Intell. 13 (6), 583–598. https://doi.org/10.1109/34.87344.
Walker, B., Holling, C.S., Carpenter, S.R., Kinzig, A., 2004. Resilience, adaptability, and transformability in social–ecological systems. Ecol. Soc. 9 (2). https://www.jstor.org/stable/26267673.
Weatherspoon, C.P., Skinner, C.N., 1995. An assessment of factors associated with damage to tree crowns from the 1987 wildfires in Northern California For. Sci. 41 (3), 430–451.
Westman, W.E., 1978. Measuring the inertia and resilience of ecosystems. Bioscience 28, 705–710. https://doi.org/10.2307/1307321.
White, A.M., Zipkin, E.F., Manley, P.N., Schlesinger, M.D., Fenton, B., 2013. Conservation of avian diversity in the Sierra Nevada: Moving beyond a single-species management focus. PLoS One 8 (5), e63088. https://doi.org/10.1371/journal.pone.0063088.
Wiggins, H.L., Nelson, C.R., Larson, A.J., Safford, H.D., 2019. Using LiDAR to develop high-resolution reference models of forest structure and spatial pattern. For. Ecol. Manag. 434, 318–330. https://doi.org/10.1016/j.foreco.2018.12.012.
Williams, A.P., Abatzoglou, J.T., Gershunov, A., Guzman-Morales, J., Bishop, D.A., Balch, J.K., Lettenmaier, D.P., 2019. Observed impacts of anthropogenic climate change on wildfire in California. Earths Future 7 (8), 892–910. https://doi.org/10.1029/2019EF001210.
Williams, J.N., Safford, H.D., Enstice, N., Steel, Z.L., Paulson, A.K., 2023. High-severity burned area and proportion exceed historic conditions in Sierra Nevada, California, and adjacent ranges. Ecosphere 14 (1), e4397.
Wood, C.M., Jones, G.M., 2019. Framing management of social-ecological systems in terms of the cost of failure: the Sierra Nevada, USA as a case study. Environ. Res. Lett. 14 (10), 105004 https://doi.org/10.1088/1748-9326/ab4033.
Young, J.D., Evans, A.M., Iniguez, J.M., Thode, A., Meyer, M.D., Hedwall, S.J., McCaffrey, S., Shin, P., Huang, C.-H., Young, J.D., et al., 2020. Effects of policy change on wildland fire management strategies: Evidence for a paradigm shift in the western US? Int. J. Wildland Fire 29 (10), 857–877. https://doi.org/10.1071/WF19189.
Zald, H.S.J., Gray, A.N., North, M., Kern, R.A., 2008. Initial tree regeneration responses to fire and thinning treatments in a Sierra Nevada mixed-conifer forest, USA. For. Ecol. Manag. 256 (1), 168–179. https://doi.org/10.1016/j.foreco.2008.04.022.
Ziegler, J.P., Hoffman, C., Battaglia, M., Mell, W., 2017. Spatially explicit measurements of forest structure and fire behavior following restoration treatments in dry forests. For. Ecol. Manag. 386, 1–12. https://doi.org/10.1016/j.foreco.2016.12.002.
Ziegler, J.P., Hoffman, C.M., Collins, B.M., Knapp, E.E., Mell, W.R., 2021. Pyric tree spatial patterning interactions in historical and contemporary mixed conifer forests, California, USA. Ecol. Evol. 11 (2), 820–834. https://doi.org/10.1002/ece3.7084.